Manufacturability and Reliability Screening of Lower Melting Point Pb-Free Alloys Containing Bi

Polina Snugovsky, Eva Kosiba, Jeffrey Kennedy, Zohreh Bagheri, Marianne Romansky

Celestica Inc.
Toronto, ON, Canada
polina@celestica.com

Michael Robinson, Joseph M. Juarez, Jr., Joel Heebink
Honeywell
AZ, US
mike.robinson6@honeywell.com
joseph.juarez@honeywell.com

Abstract

This paper is the first of two papers discussing the Celestica/Honeywell Lower Melt Alloy program. The program explores the manufacturability and reliability for Pb-freethree Bi-containing alloys in comparison with conventional SAC305 and SnPb assemblies. The first alloy included in the study is a Sn-based alloy with 3.4%Ag and 4.8%Bi which showed promising results in the National Center for Manufacturing Sciences (NCMS) and German Joint (GJP) projects. The other two alloy variations have reduced Ag content, with and without Cu.

BGA and leaded components were assembled on medium complexity test vehicles using these alloys, as well as SAC305 and SnPb as base line alloys for comparison. Test vehicles were manufactured using two board materials, 170°C glass transition temperature (Tg) and 150°C Tg, with three surface finishes: ENIG, ENEPIG, and OSP. The ATC testing was done at -55°C to 125°C with 30 minute dwells and 10C/min ramps. Vibration at two G-Force test conditions with resistance monitoring was performed. In this paper, the detailed microstructure examination before testing and after 1500 cycles of -55°C to 125°C, together with failure analysis, is described. These results allow preliminary recommendations of proper combinations of the solder alloys, board materials, and surface finishes for high reliability applications.

Key words: Lower Melt Pb-free solder, Bi-containing alloys, metallurgical analysis, thermo-mechanical reliability, vibration

Introduction

Aerospace and Military companies continue to exercise RoHS exemptions and to intensively research long term attachment reliability for RoHS compliant solders. Their products require higher vibration, and drop/shock performance, and combined-environment reliability than the conventional SAC305 alloy provides. The NASA-DoD Lead-Free Electronics Project confirmed that pad cratering is one of the dominant failure modes that occur in various board level reliability tests, especially under dynamic loading [1].

One possible rout to improvement of the mechanical and thermo-mechanical properties of solder joints is the use of Pb-free solders with lower process temperatures. Lower temperatures help to reduce the possibility of damaging the boards and components, and also may allow the use of lower Tg board materials which are less prone to pad cratering defects. There are several Sn-Ag-Bi and Sn-Ag-Cu-Bi alloys which melt about 10°C lower than SAC305. The Bismuth in these solder compositions not only reduces the melting temperature, but also improves thermo mechanical behavior [2-4]. An additional benefit of using Bi-containing solder alloys is the possibility to reduce the propensity to whisker growth [5].

Several ternary SnAgBi and quaternary SnAgCuBi Pb-free solder alloys have shown great mechanical and thermo-mechanical reliability in previously completed projects: National Center for Manufacturing Sciences (NCMS) [6] and JCAA/JGPP Lead-Free Solder Project [7] and new studies (GJP Lead-Free Avionics) recently presented at the Aerospace Industry Association (AIA) PERM meeting [8]. Some of these Pb-free alloys have melting temperatures comparable to SnPb, allowing for the use of SnPb processing temperatures for Pb-free assemblies. Some alloys may have a lower Ag content that will reduce the solder cost and contribute to mechanical improvement in properties.

Celestica, in a partnership with the University of Toronto, has been working on a project with the objective of selecting new Pb-free alloys with process temperatures comparable to conventional SnPb solder for assembly and rework of ball grid array and leaded and pin-through-hole components since 2009 [9]. From an initial list of 23 alloys studied for metallurgical performance, a total of seven SnAgBi and SnAgCuBi alloys were selected for screening experiments of mechanical and thermo-mechanical properties. Some of the alloys showed good manufacturability and drop test performance.

Alloys containing Bi have not been widely utilized due to the formation of a low melting ternary SnPbBi alloy when SnAgCuBi solder joints are contaminated with Pb from SnPb component finishes. With the increased use of lead-free solder alloys and components finishes, SnPb component finishes are becoming obsolete, reducing the risk of Pb contamination of Bi-containing solder alloys.

This paper is the first of two papers discussing the Celestica/Honeywell Lower Melt Alloy program. The program explores the manufacturability and reliability screening results for the three Bi-containing alloys in comparison with conventional SAC305 and SnPb assemblies.

Experimental

Alloy selection

Three alloys out of seven analyzed in the Celestica/U of T study [9] were selected for the high reliability environment testing. The alloy names, constituent elements, minimum melting temperatures and melting temperature ranges are shown in Table 1.

Table 1: Alloy Selected for High Reliability Screening Experiments

#	Celestica Name	Alloy constituents	Alloy composition	Min Melting Temperatures, °C (Experimental)	Melting Range, °C
1	Paul	SnAgBi	Sn3.4%Ag4.8%Bi	206	11
2	Violet	SnAgCuBi	Sn2.25%Ag0.5%Cu6.0%Bi	205	10
3	Orchid	SnAgBi	Sn2.0%Ag7.0%Bi	190	25
4	SAC305	SnAgCu	Sn3.0%Ag0.5%Cu	217	6
5	Eutectic SnPb	SnPb	Sn37.0%Pb	183	0

Alloy #1 “Paul” was proposed by Paul Vianco. Excellent thermo mechanical properties for harsh environments were proved by NCMS [6] and the German Joint Lead-Free Avionics project [8]. Alloys #2 and #3 are modifications of the “Paul” alloy.

Alloy #2 “Violet” has a lower Ag content and does not form Ag_3Sn plates. It may help to improve drop/shock properties. Cu is added to the formulation to reduce the Cu dissolution potential. The optimized Bi content related to reduce Ag may help to better mitigate whisker formation and to slightly lower the melting temperature compared to the “Paul” alloy. Both alloys have an excellent pasty range.

Alloy #3 “Orchid” is a variant of the “Paul” alloy, with lower Ag and higher Bi content, which allows the significant reduction of the minimum melting temperature. The pasty range is wider than in alloys #1 and #2. Because of a lower melting temperature and higher Bi content, it may dissolve even less Cu and provide greater whisker mitigation than Alloy #1 “Paul”.

SAC305 and Sn-Pb solders were included in the test matrix for comparison.

No-clean solder pastes of the experimental alloys were produced by one of the major solder paste suppliers. The solder paste performance evaluation was done using a Celestica test vehicle and a standard Celestica solder paste evaluation procedure [10].

Statistical considerations

The ATC experiment is summarized in Table 1. To compare the several combinations of solder paste, substrate finish, and T_g, two design experimental matrices were chosen; full factorial as found, and a Latin Square as illustrated in Table 2 and Table 3.

Specifically, the Latin square design of order three is shown below. In general, the rows represent levels of one factor, the columns, another factor, and numbers in the cells, levels of a third factor. The Latin Square is a subset of all possible combinations where each level of one factor is present with each level of another factor. The advantage is that the Latin Square provides estimates of factor level differences in a fraction of the possible combinations. In this case, the Latin Square of order 3 uses 9 combinations rather than the 27 required for a full factorial experiment [11].

Table 1: Experimental Design using Three Factors Applied to the Failure of Six Components Using a Latin Square for Run Combinations 1-9 and a Full Factorial for Runs 10-17

Paste type	Paul			Violet			Orchid			SAC305				Sn-Pb			
Finish	OSP	ENIG	ENEPIG	OSP	ENIG	ENEPIG	OSP	ENIG	ENEPIG	OSP	OSP	ENEPIG	ENEPIG	OSP	OSP	ENEPIG	ENEPIG
T_g	150	170	170	170	150	170	170	170	150	150	170	150	170	150	170	150	170
Component Type	1	2	3	4	5	6	7	8	9	10	11	12	13	14	15	16	17
352 BGA	/02	/02	/02	/02	/02	/02	/02	/02	/02	/02	/02	/02	/02	/02	/02	/02	/02
240 QFP	/02	/02	/02	/02	/02	/02	/02	/02	/02	/02	/02	/02	/02	/02	/02	/02	/02
SSOP 48	/06	/06	/06	/06	/06	/06	/06	/06	/06	/06	/06	/06	/06	/06	/06	/06	/06
PLCC 84	/06	/06	/06	/06	/06	/06	/06	/06	/06	/06	/06	/06	/06	/06	/06	/06	/06
SO 20	/08	/08	/08	/08	/08	/08	/08	/08	/08	/08	/08	/08	/08	/08	/08	/08	/08
SOJ 40	/08	/08	/08	/08	/08	/08	/08	/08	/08	/08	/08	/08	/08	/08	/08	/08	/08

Table 2: General Latin Square

	a	b	c
A	1	2	3
B	3	1	2
C	2	3	1

The T_g factor only has two levels of interest so the high level was duplicated as the middle level. This is a common practice when one factor has fewer levels than the other two and presents only a minor complication in the analysis. Essentially, the difference between the high and middle levels is known to be equal to zero.

Table 3: Latin Square of Paste and Finish

		Finish		
		OSP	ENIG	ENEPIG
PASTE	Paul	150	170	170
	Violet	170	150	170
	Orchid	170	170	150

The factorial portion uses factors relevant to the traditional tin-lead pastes. In this case, each factor only had two levels of interest so the traditional 2x2x2 layout was used.

The run data is summarized as pass/fail in Table 1 with all components combined together. The resulting response is proportion, $p = x/n$, of n samples that are defective. This is modeled using the binomial distribution. Unfortunately, this response is known to exhibit the complication of non-constant variance across inference space. The proportions are transformed using the Freeman-Tukey adaptation of the arcsine of the proportion to stabilize the variance across the treatment combinations. Then, the usual Analysis of Variance may be used to evaluate factor and level effects.

It is anticipated that the data on individual components will result in time to failure data. These data will be analyzed by fitting failure time distributions and applying a regression model.

Test vehicle

The test vehicle was designed by Honeywell and has been used for numerous Tin Lead baseline and Lead Free process development activities. The assembly and reflow processes at Celestica Toronto's Process Development Center have been optimized to accommodate the assembly of various daisy chained SAC 305 BGAs and Matte Tin leaded components. The board stack up and dimensions are representative of a large percentage of aerospace products and designed per IPC-4101/126 &/129 requirements. Assembling this well characterized board in a variety of board finishes while processing duplicate sets of components should make the comparison of various Low Melt Lead Free alloys easier.

<u>Board materials</u>

The objective of testing different laminate materials was to see if there was any pad cratering benefit when using a lower Tg material enabled by the lower process temperature. This lower Tg in combination with the low melt alloy was expected to deliver equal or better performance at a potentially lower cost point.

Table 5: Laminate materials

Tg (°C)	LAMINATE	SUPPLIER
150	Nelco 4000-7	Holaday Circuits
170	Isola 370HR	Holaday Circuits

Board surface finishes

Multiple surface finishes were used to compare soldering performance at various metallic interfaces to review performance when soldered to Copper or Nickel.

Table 6: Surface finishes

SURFACE FINISH	THICKNESS (µm)
OSP	Entek 106A (Copper Triazole)
ENIG	MacDermid Ni 3.81µm - 0.13-0.20µm Au
ENEPIG	Uyemura Ni 3.81µm – 0.05µm Pd – 0.08µm Au

Dimensions and number of layers

The overall dimensions for the PWB test vehicle are approximately; 203mm x 355mm and 2.5mm thick with 16 layers of alternating signal and ground/power plane with copper. All of the wiring on the PWB is to accommodate daisy chain active resistance monitoring and output to an edge connector pattern for wiring. Below is a photo of the Test vehicle layout. It includes packages that represent the variety typically seen on products.

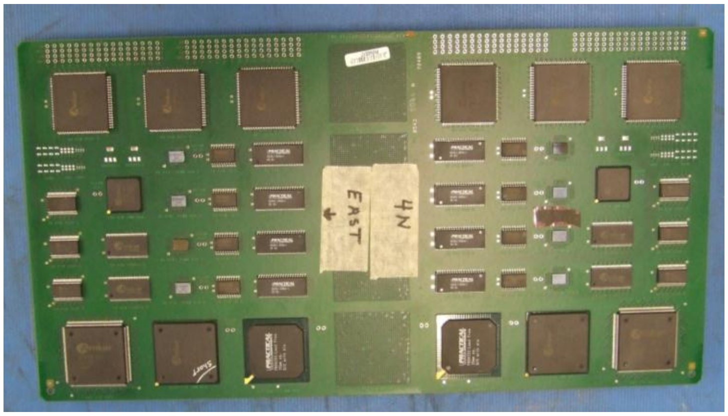

Figure 1: Test vehicle

The package types, component dimensions, I/O counts, solder ball composition, and lead finishes are shown in Table 7.

Table 7: Component types

I/O COUNT/ PACKAGE	DIMENSIONS	PITCH	LEAD FINISH	BALL COMPOSITION
20 /SO	6.35 X 12.70 mm	1.27 mm	Sn-Pb and Matte Tin	
40 /SOJ	10.16 X 25.40 mm	1.27 mm	Sn-Pb and Matte Tin	
48 /SOP	5.08 X 15.24 mm	0.50 mm	Sn-Pb and Matte Tin	
54 /TSSOP	10.16 X 21.59 mm	0.64 mm	Sn-Pb and Matte Tin	
84 /PLCC	29.21 X 29.21 mm	1.27 mm	Sn-Pb and Matte Tin	
240/ PQFP	31.75 X 31.75 mm	0.50 mm	Sn-Pb and Matte Tin	
289 /BGA	17.15 X 17.15 mm	1.02 mm		SAC 305
352 /BGA	35.56 X 35.56 mm	1.27 mm		SAC 305
1156/ BGA	34.93 X 34.93	1.02 mm		SAC 305

These partially assembled boards were continuously monitored with Anatech resistance event detection equipment during Harsh Environment accelerated thermal cycling and vibration exposures representative of product requirements. The range of component type, size, and board finishes provide a comprehensive look at selected lower melt Pb-Free alloys that can be compared to SAC 305 and SnPb baseline test data.

This screening experiment defines the critical variables and provides a path for more an in-depth study of low melt solders while minimizing the costs. Our hope is that this work will lead to some interesting results which can then be leveraged by the industry to further evaluate the lower melt alloys.

Assembly

Fifty six of the above test vehicles were built at Celestica between March 22 and March 29, 2012 using different combinations of board material, surface finish and alloys according to Table 8.

Table 8: Build Matrix

Board Material	Alloy	Surface Finish		
		ENEPIG	ENIG	OSP
Normal T_g	SnPb	2		3
	SAC305	2		2
	Paul			4
	Violet		4	
	Orchid	4		
High T_g	SnPb	2		3
	SAC305	2	1	3
	Paul	4	4	
	Violet	4		4
	Orchid		4	4

Seven thermocouples were placed on the board at various locations, both on components and on the board itself in order to determine the optimal profiles. Two profiles were used; one with a peak reflow temperature of 240°C used for SAC305 and one with a peak reflow of 222°C, which was used for all other alloys. In both cases the time above liquidus was between 70 and 90 seconds. The profiles are shown in **Error! Reference source not found.** and **Error! Reference source not found.** respectively. All boards where reflowed in a 10-zone Electovert Omniflow oven.

During the solder screening process, solder paste heights and volumes were measured. Every attempt was made to print equal volumes using each of the various solder pastes. All components were placed using a Siemens Siplace X3 SMT placement machine with a standard nozzle. Visual and XRay inspections were then performed on each of the assembled boards. Additionally, one board was sent for cross sectioning to ensure the appropriateness of the profiles prior to completion of the build.

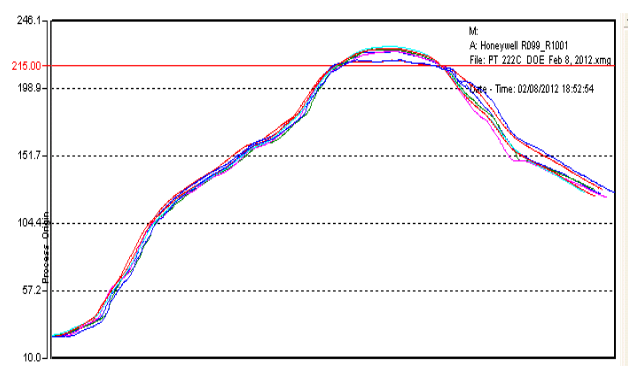

Figure 2: Reflow Profile for 240°C

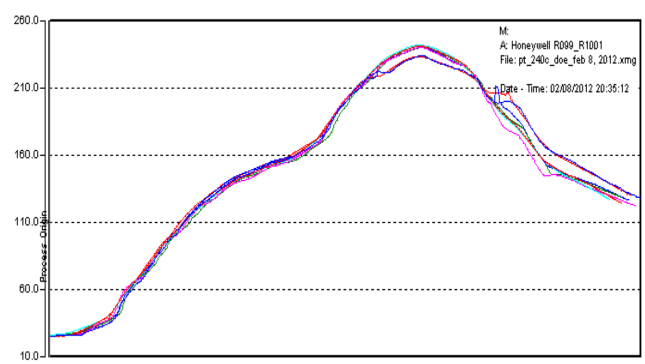

Figure 3: Reflow Profile for 222°C

Accelerated Temperature Cycling

17 boards were exposed to Accelerated Temperature Cycling (ATC). ATC was performed to a target of -55°C to 125°C with a ramp rate of 10°C/min and a 30 minute dwell at both extremes. Temperature measurements for guiding the profile were measured at the test vehicle component level as opposed to the chamber level. The actual profile resulted in a hot dwell at 130°C for 38 minutes and a cold dwell at -58°C for 39 minutes with a 13 minute ramp in between, totaling 103 minutes per cycle as shown in Figure 5. Boards were placed into two racks within the chamber, as seen in Figure 4 to allow the air to circulate freely. At the time that this paper was written, 2001 cycles were complete. The test will continue to a total of 3000 cycles.

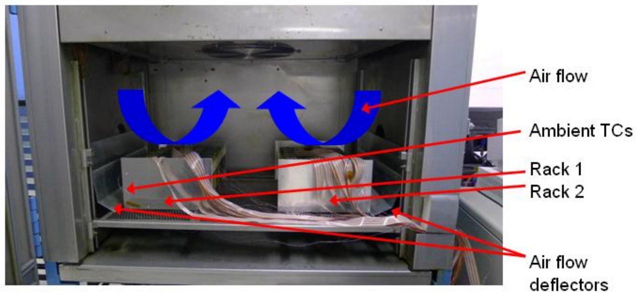

Figure 4: ATC Chamber Set Up

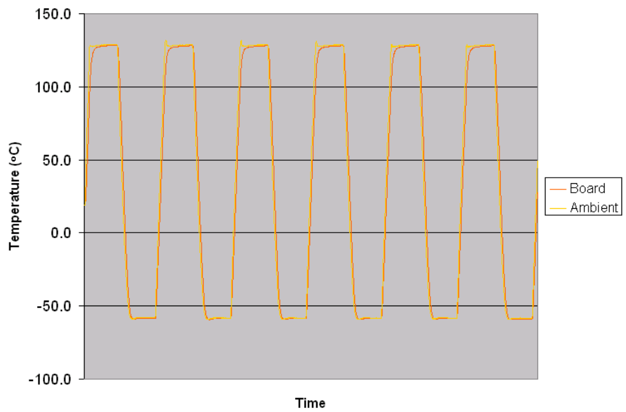

Figure 5: ATC Profile

Analysis Tech STD-256 event detectors were used to monitor the resistance thresholds of 32 components on each board. A failure was recorded when the channel resistance increased to 300W or more for at least 200ns. Each recorded failure was checked at room temperature to determine the location of failure, i.e. within the component, a board ortrace issue or within the cable connection. Selected failed components were cut from the board for detailed analysis, while the remaining components were returned to the chamber for further testing.

Vibration testing plan

26 boards were subjected to vibration testing; 17 at a 5G level and 9 at a 2G level. Resistance, strain and vibration were recorded. Component failure was determined through resistance monitoring using the same method described in the ATC testing. Strain was monitored at regular intervals throughout the test on a representative sample size of boards. Vibration was monitored using an accelerometer at the centre of each board, the area that would experience the most flexure. Figure 6 shows 4 boards installed in the fixture with the various monitoring systems.

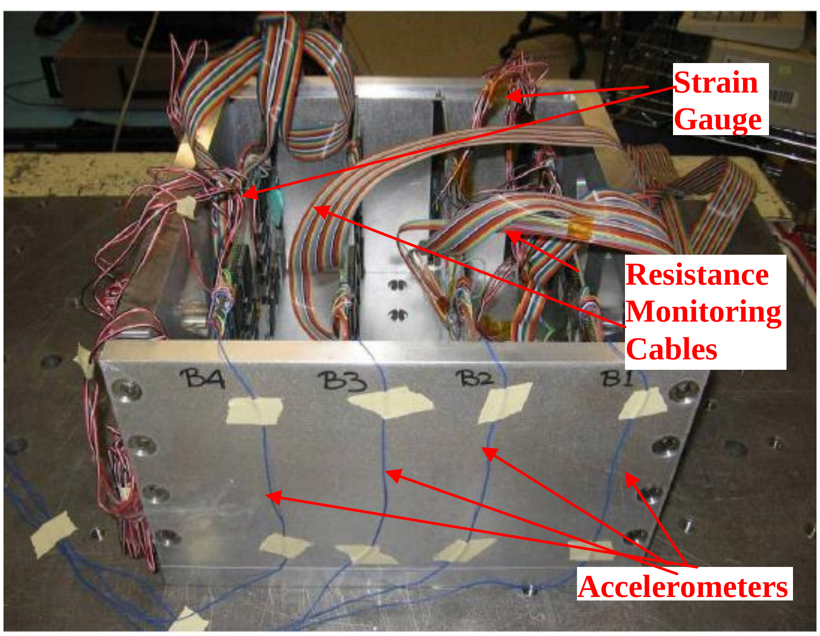

Figure 6: Vibration Fixture with Boards

An attempt was made to group boards of the same material and similar finish/alloy combinations together in a group for testing. A summary of the grouping can be found in Table 4.

Table 4: Vibration Test Parameters per Group

T_g / Alloy / Finish		Location			
Vibration Level	**Group**	**B1**	**B2**	**B3**	**B4**
5G	1	170 / Violet / ENEPIG*	170 / Paul / ENIG	170 / SAC305 / ENEPIG	170 / Sn-Pb / ENEPIG
	2	170 / Paul / ENEPIG**	170 / Sn-Pb / OSP		
	3	170 / Orchid / ENIG*	170 / Violet / OSP	170 / SAC305 / OSP	170 / Orchid / OSP*
	4	150 / Orchid / ENIG*	150 / SAC305 / OSP	150 / SnPb / OSP	
	5	150 / Violet / ENIG**	150 / SAC305 / ENEPIG	150 / SnPb / ENEPIG	150 / Orchid / ENEPIG**
2G	6	150 / Paul / OSP	150 / Violet / ENIG	150 / Orchid / ENEPIG	
	7	170 / Paul / ENIG	170 / Violet / ENEPIG	170 / Orchid / OSP	
	8	170 / Paul / ENEPIG	170 / Violet / OSP	170 / Orchid / ENIG	

Indicates that strain gauge scenario 1 was used (as seen in Figure 7). ** Indicates that strain gauge scenario 2 was used (as seen in **Error! Reference source not found.**). Since only boards which were used for 5G testing had strain gauges attached, these boards were exposed to both a sine sweep at 2G and 5G in order to best characterize the boards at both G levels. The boards used for 2G testing were only exposed to a 2G sine sweep in order to determine the appropriate resonant frequencies. After the sine sweeps, the group of boards was then exposed to approximately 6 hours of sine dwell at the assigned vibration levels.

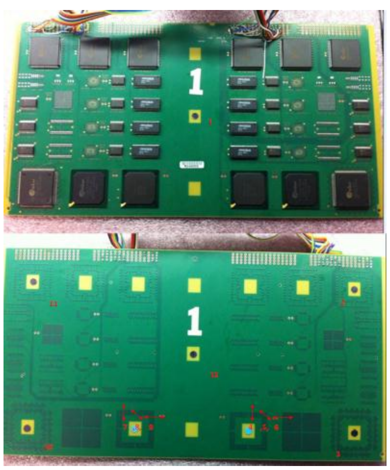

Figure 7: Vibration Strain Gauge Location Scenario 1 (showing both front and back of board)

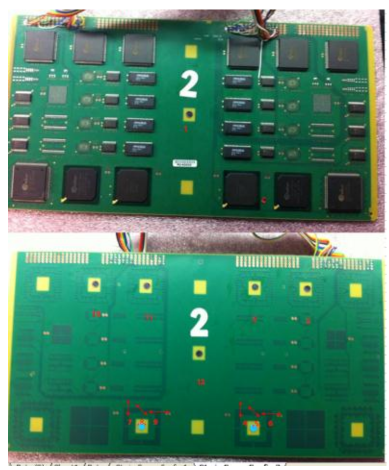

Figure 8: Vibration Strain Gauge Location Scenario 2 (showing both front and back of board)

Metallurgical analysis after assembly and Failure Analysis

Optical microscopy, X-ray (Phoenix PCB analyzer), scanning electron microscopy (SEM, Hitachi S-4500 and SEM Hitachi S-3000N), and X-ray spectroscopy (Oxford EDX) were used for solder joint quality and microstructure analysis.

BGA352 location U200, was exposed to the lowest temperature during reflow, and QFP240 location U23, which experienced the hottest temperature, were cross-sectioned to analyze the microstructure and measure the intermetallic reaction layer. For the Lower Melting temperature alloy profile, the lowest temperature of the center and the corner balls of the BGAs were 224.9°C and 227.5°C, respectively. The BGA cross-sectioning was done diagonally. The peak temperature on the QFPs was 232°C. Twelve boards were cross-sectioned and analyzed.

Results and Discussion

As assembled solder joint quality and microstructure

All assemblies had acceptable solder joints in terms of voiding, wetting, shape, and size. No major anomalies or concerns were noted. The maximum void percentage of the BGA352 ball is shown in Table 10. Experimental alloys have less voiding than SAC305 and comparable to SnPb. The lower level of voiding is found on ENEPIG followed by ENIG and then OSP. The typical X ray images of voiding are shown in Figure 1. Wetting on OSP that may be a problem with SAC305 is improved for the experimental alloys containing Bi (Fig.9).

Table 10: Voiding in BGA352

Assembly #	Solder Name	Surface	Voiding,%
1	Tin-Lead	OSP	15.7
2	SAC305	OSP	24.5
3	Paul	OSP	17.7
4	Violet	OSP	22.0
5	Orchid	OSP	17.2
6	SAC305	ENIG	23.2
7	Paul	ENIG	13.0
8	Violet	ENIG	12.1
9	Orchid	ENIG	12.9
10	Paul	ENEPIG	10.5
11	Violet	ENEPIG	3.5
12	Orchid	ENEPIG	10.7

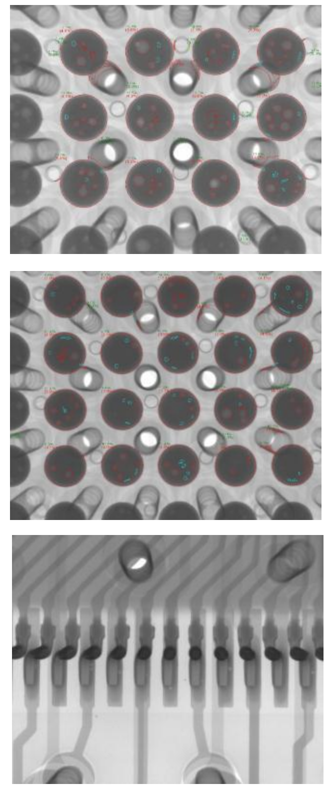

Figure 9: Examples of voiding in experimental assembles: top – BGA352 Violet on OSP; centre – BGA352, SAC305 on OSP; bottom – QFP204, Paul on OSP

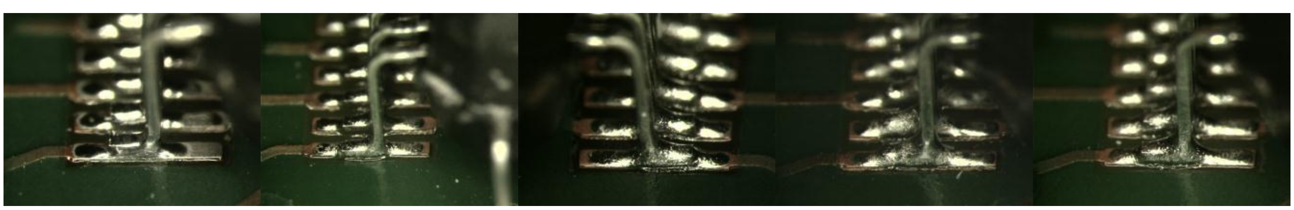

SnPb SAC305 Paul Violet Orchid

Figure 10.Example of wetting on OSP, QFP240: A – SnPb; B – SAC305; C – OSP; D – Violet; E - Orchid

Cross-sections of BGA325 and QFP240 illustrating a proper solder joint shape are shown in Figure 11. SAC305 solder balls were completely mixed with Bi containing solders. The resulting composition was analyzed using EDX as shown in Figure 12. This example demonstrates a BGA325 solder joint with SAC305 ball reflowed on an OSP board using Paul solder paste. Although the semi-quantitative EDX analysis does not give a precise solder composition, it allows a comparison of solder joints formed on different surface finishes using different alloys (Table 11). The trend of reducing Ag content when SAC 305 ball is mixed with lower Ag alloys Violet and Orchid is visible. The Cu content depends on the surface finish. The Cu is slightly lower on ENIG and ENEPIG when the joint is formed using no-Cu alloys Paul and Orchid. Cu dissolves in solder joints formed on OSP finished boards; even SnPb joints contain 0.4%Cu. The Cu content in Pb-free joints formed on OSP boards is about two times higher compared to the joints formed on ENIG and ENEPIG boards.

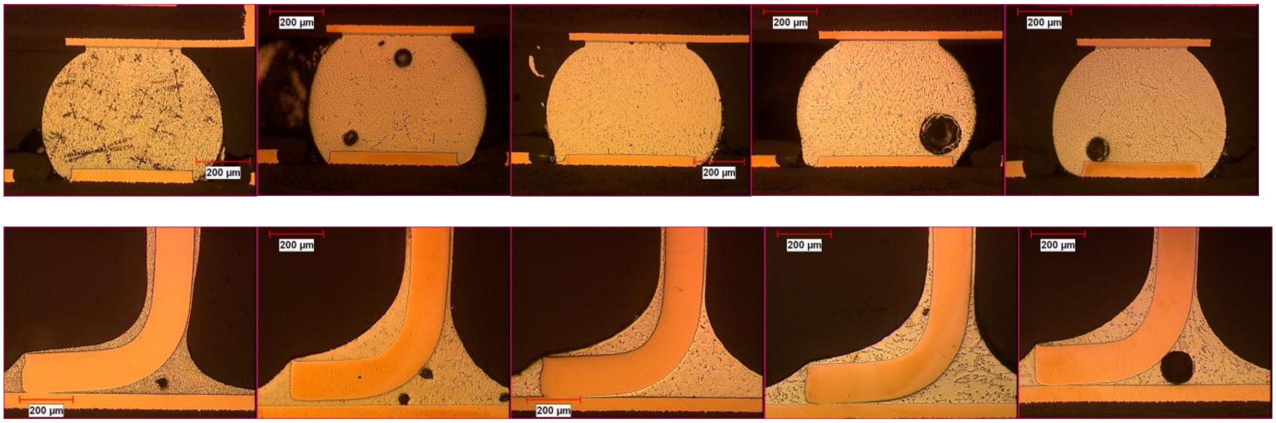

SnPb SAC305 Paul Violet Orchid

Figure 11:BGA325 and QFP240 structure, OSP, 100x

The Bi content in BGAs is similar in all three experimental alloys and does not exceed 2.1%. The Bi content was also measured in Sn grains. The ion beam was placed in the Sn location clear of on any visible precipitations. The results are shown in Table 4. The Bi in Sn grains is also about 2 wt% (1at %). This amount of Bi is very close to the solubility in Sn at the ambient condition (Fig. 13) and will provide solid-solution strengthening. Therefore, Bi precipitation is not expected in BGA solder joints.

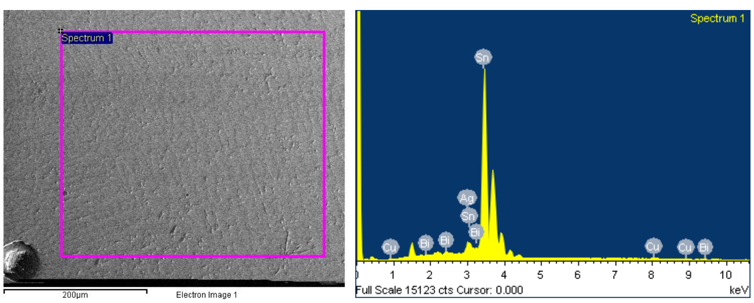

Element	Weight%	Atomic%
Cu K	0.8	1.6
Ag L	2.6	2.9
Sn L	94.9	94.6
Bi M	1.7	0.9
Totals	100.0	

Figure 12: EDX Analysis of BGA325 formed on OSP using Paul solder paste, 100x

Table 11: BGA352 Composition

Assembly #	Solder Name	Surface finish	BGA Composition				
			Sn	Ag	Cu	Bi	Pb
1	Tin-Lead	OSP	70.2	0	0.4	0	29.4
2	SAC305	OSP	96.2	2.8	1.0	0	0
3	Paul	OSP	95.0	2.6	0.8	1.7	0
4	Violet	OSP	95.7	2.1	0.7	1.5	0
5	Orchid	OSP	94.7	2.3	1.0	2.0	0
6	SAC305	ENIG	96.7	2.8	0.5	0	0
7	Paul	ENIG	95.9	3.0	0.3	0.8	0
8	Violet	ENIG	95.5	2.2	0.6	1.7	0
9	Orchid	ENIG	95.0	2.5	0.4	2.1	0
10	Paul	ENEPIG	95.0	2.5	0.4	2.1	0
11	Violet	ENEPIG	95.1	2.8	0.6	1.5	0
12	Orchid	ENEPIG	95.5	2.2	0.4	1.9	0

Table 12: Bi content in Sn grains

Assembly #	Solder Name	Surface finish	QFP		BGA	
			Wt %	At %	Wt %	At %
1	Tin-Lead	OSP	0	0	0	0
2	SAC305	OSP	0	0	0	0
3	Paul	OSP	3.1	1.8	1.5	0.9
4	Violet	OSP	3.8	2.2	1.4	0.8
5	Orchid	OSP	3.8	2.2	2.1	1.2
6	SAC305	ENIG	0	0	0	0
7	Paul	ENIG	3.8	2.2	1.2	0.7
8	Violet	ENIG	3.7	2.1	1.9	1.1
9	Orchid	ENIG	4.1	2.4	2.4	1.4
10	Paul	ENEPIG	4.0	2.3	2.0	1.1
11	Violet	ENEPIG	3.5	2.0	2.0	1.1
12	Orchid	ENEPIG	3.5	2.0	1.6	0.9

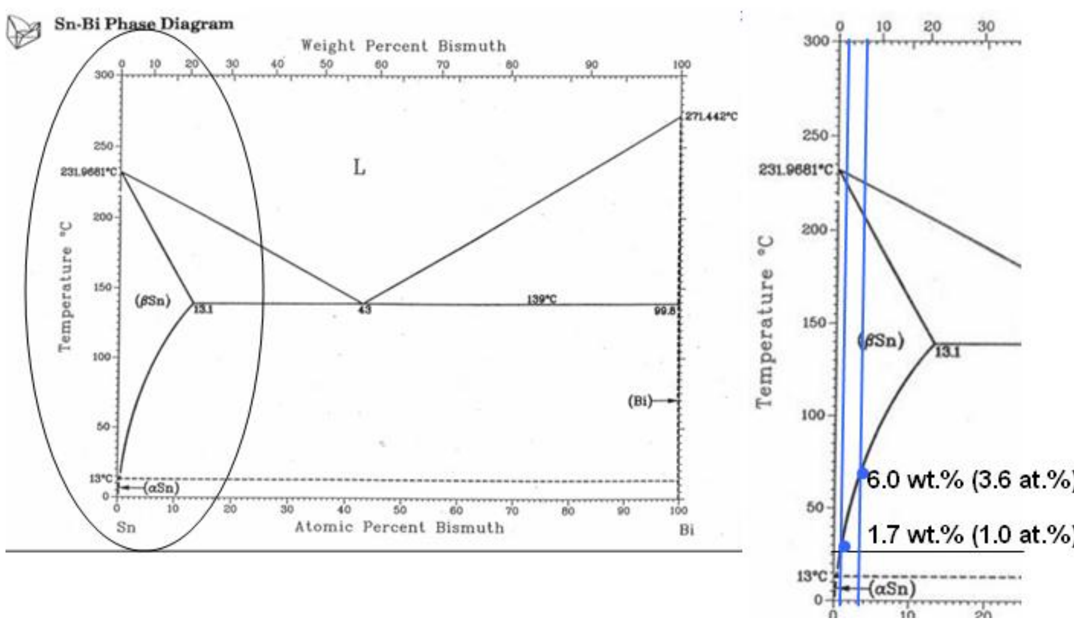

Figure 13: Sn-Bi phase diagram showing Bi dissolution at different temperature

The representative microstructures of the BGA352 solder joints are shown in Figure 14. The experimental alloys have microstructure similar to SAC305 with primary-like Sn dendrites and interdendritic eutectic: Ag_3Sn + Sn or Ag_3Sn + Cu_6Sn_5 + Sn. The diameter of Sn dendrite branches is smaller in SAC305 than in all three Bi containing alloys. The dendritic structure in OSP joints is finer than in ENIG and ENEPIG joints. No Bi precipitation was detected in BGA352.

The Sn grains in QFP240 joints contain 3 to 4 wt% Bi (Table 12), which is about 2 time higher Bi dissolution limit at room temperature. The Bi is expected to precipitate in a Sn matrix and cause solid-solution and precipitation strengthening effect. A typical microstructure of the experimental Bi-containing alloys is shown in Figure 8. The microstructure contains primary Sn dendrites and interdendritic eutectic: Ag_3Sn + Sn or Ag_3Sn + Cu_6Sn_5 + Sn. The Bi particles are found in the eutectic regions and inside the primary Sn grains. The dendritic structure of the QFP240 joints is also coarser in experimental alloys than in SAC305.

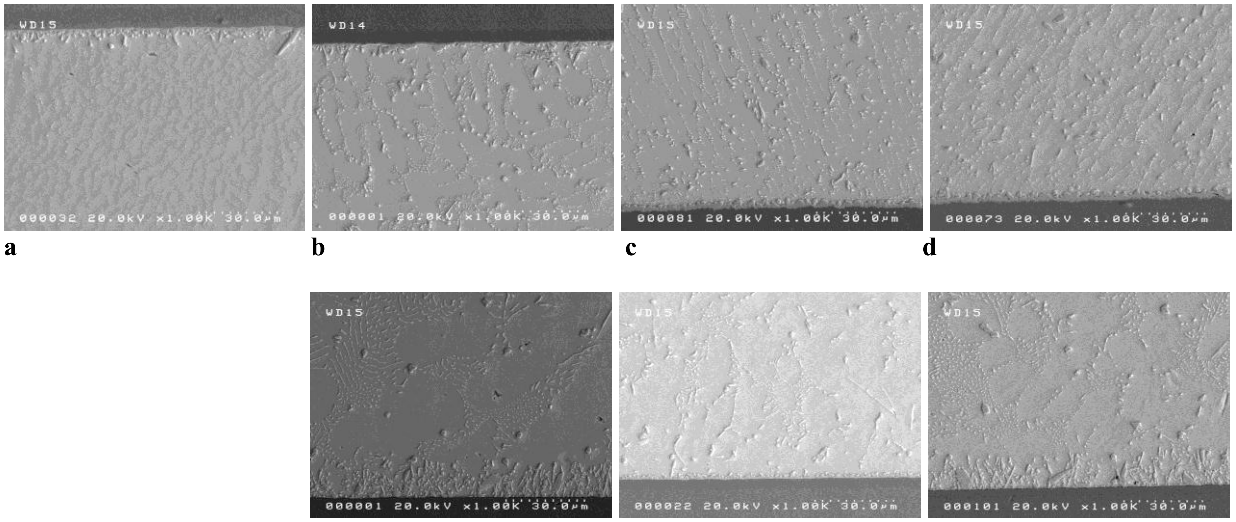

a b c d

e f g

Figure 14: Microstructure of BGA352 solder joints, SEM, 1000x : a – SAC305, OSP; b - Paul, OSP; c - Violet, OSP; d – Orchid, OSP; e - Paul, ENEPIG; e - Violet, ENEPIG; e - Orchid, ENEPIG;

.

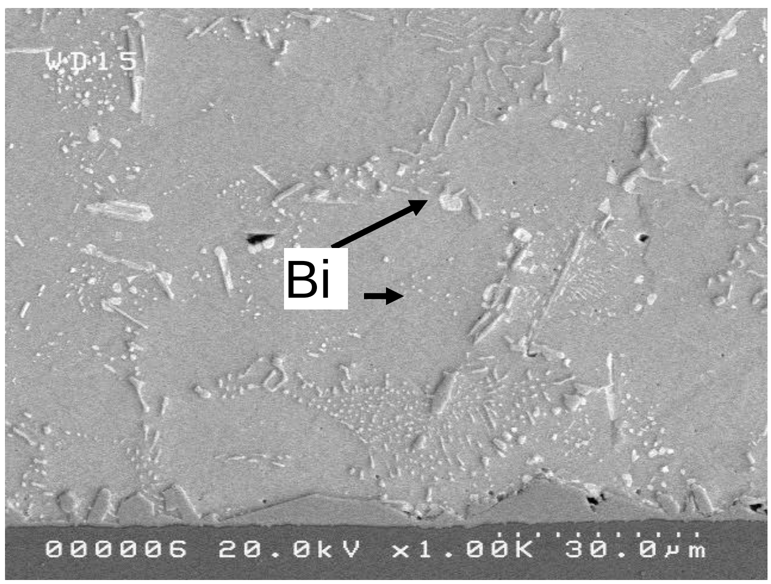

Figure 15: Microstructure of QFP240 solder joints, Paul, ENEPIG, SEM, 1000x

The intermetallic thickness was measure on both board and component sides in BGA352 and QFP240. The results are shown in Table 13. The intermetallic morphology on the board side is shown in Figures 16 and 17. In most BGA and all QFP solder joints formed on OSP, ENIG, and ENEPIG surface finishes using SnPb, SAC305, and the three alloys containing Bi, the intermetallic does not exceed 3.9µm. The intermetallic in Paul and Orchid BGAs on ENEPIG board side is very thick. Because of the irregular shape, it cannot be properly measured.

Excluding Paul and Orchid on ENEPIG, the thickest intermetallic in BGAs grows in SAC305 joints on OSP surface finish. This thickness is attributed to the higher reflow process temperature. In QFPs, the thickest intermetallic is formed in Orchid. This alloy has the widest pasty range and remains in liquid stage for a longer time during reflow. The intermetallic in Paul is in a thicker range compared to Violet. The intermetallic in Violet is always thinner and properly formed, and the same thickness on all surface finishes. Only the Violet intermetallic layer has a regular proper shape on the ENEPIG finish (Fig. 16 and 17).

Table 13: Intermetallic thickness

Assembly #	Solder Name	Surface finish	QFP IMC thickness, µm		BGA, IMC thickness, µm	
			Board	Component	Board	Component
1	Tin-Lead	OSP	1.8	2.0	2.2	2.1
2	SAC305	OSP	2.1	2.5	3.3	2.4
3	Paul	OSP	1.9	1.9	2.4	1.5
4	Violet	OSP	1.9	2.2	2.1	1.7
5	Orchid	OSP	2.0	2.2	2.4	1.6
6	SAC305	ENIG	1.2	2.3	1.6	1.4
7	Paul	ENIG	2.1	3.6	1.0	1.3
8	Violet	ENIG	1.7	2.6	2.1	1.2
9	Orchid	ENIG	2.9	3.5	1.9	1.5
10	Paul	ENEPIG	1.5	3.5	Irregular	1.7
11	Violet	ENEPIG	1.8	2.1	1.1	0.9
12	Orchid	ENEPIG	3.9	3.2	Irregular	1.6

Solder joint properties depends, addition to its thickness, on the intermetallic type and the morphology of the interfacial layer. The morphology is deeply dependent on the intermetallic lattice and composition. The EDX analyses were performed on board and component sides of both BGA352 and QFP240. The type and the composition of the interfacial intermetallic layers are shown in Table 14. SnPb and Pb-free solders: SAC305 and three Bi-containing alloys, form Cu_6Sn_5 compound on OSP finished boards. The organic protective coating (OSP) rapidly dissolves in liquid solder and then copper dissolves in liquid tin and forms Cu_6Sn_5 . Cu_6Sn_5 (η-phase) has a hexagonal close-packed structure. In the BGAs, up to 4%Ni substitutes the Cu in the intermetallic (Fig. 18). The interfacial intermetallic layers have a typical for the Cu_6Sn_5 nodule morphology as shown in Figure 16 -18.

The intermetallic reaction layer formed between Ni/Au finished component pads and the SAC305 solder ball contained about 20 to 25 at. % Ni, 30 to 35 at. % Cu, and 42 to 45 at. % Sn and was found to be a ternary compound. The existence of this compound in a SnNiCu system was shown by Obemdorff in 2001 [12] and was confirmed by L. Snugovsky et al [13] in 2005. As shown in [12], this ternary compound corresponds to the formula $Ni_{23}Cu_{33}Sn_{44}$. This type of intermetallic forms on ENIG and ENEPIG finished boards when soldered using SAC305 or Violet. Both solders contain 0.5%Cu. The interfacial intermetallic layer has a rather smooth cellular morphology.

In BGAs assembled on ENIG boards, Paul and Orchid alloys that do not have Cu in their composition form the Ni based $(Ni,Cu)_3Sn_4$ compound. This compound is typical for Cu content lower than 0.2% [14]. The solders with lower melting temperature start forming intermetallic immediately after melting, before a SAC305 solder ball fully dissolves in liquid. The Cu introduced during mixing substitutes Ni up to 4 at. %. The $(Ni,Cu)_3Sn_4$ intermetallic layer has a sharp needle-like structure (Fig. 16).

In BGAs assembled on ENEPIG boards using Paul and Orchid alloys, in addition to the $(Ni,Cu)_3Sn_4$ compound, Pd-based intermetallic forms (Fig.19 a). This intermetallic also contains some Au, Ni and Cu atoms in a composition close to the $MeSn_4$ formula. The reaction intermetallic layers between ENEPIG and both no-Cu ternary SnAgBi alloys Paul and Orchid are extremely non-uniform, irregular in shape and have needle–like morphology (Fig. 16 and 19 a).

In QFPs assembled on ENEPIG boards, Pd is dissolved in the board and component side $(Cu,Ni,Pd)_6Sn_5$ compounds (Fig. 19 b). Pd-based needles are found in the bulk solder of all solder joints formed on the ENEPIG finished boards (Fi.19 c).

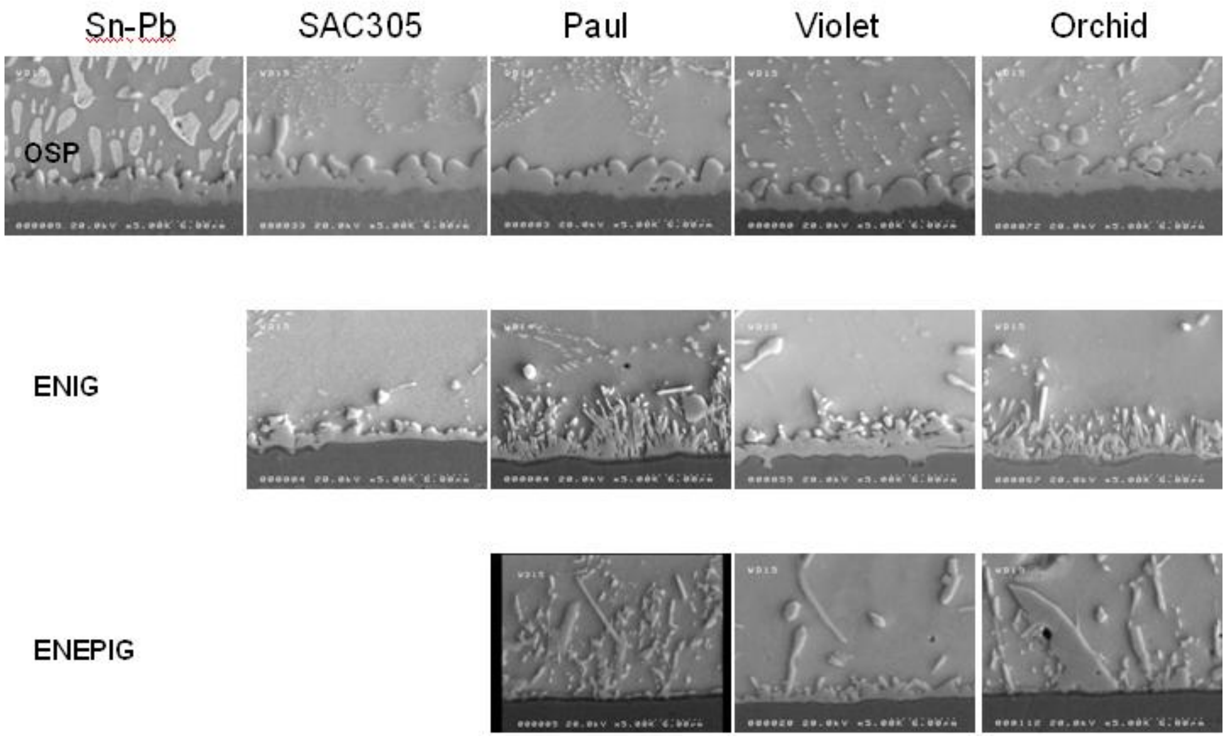

Figure 16: Intermetallic formation in BGA352, SEM, 5000x

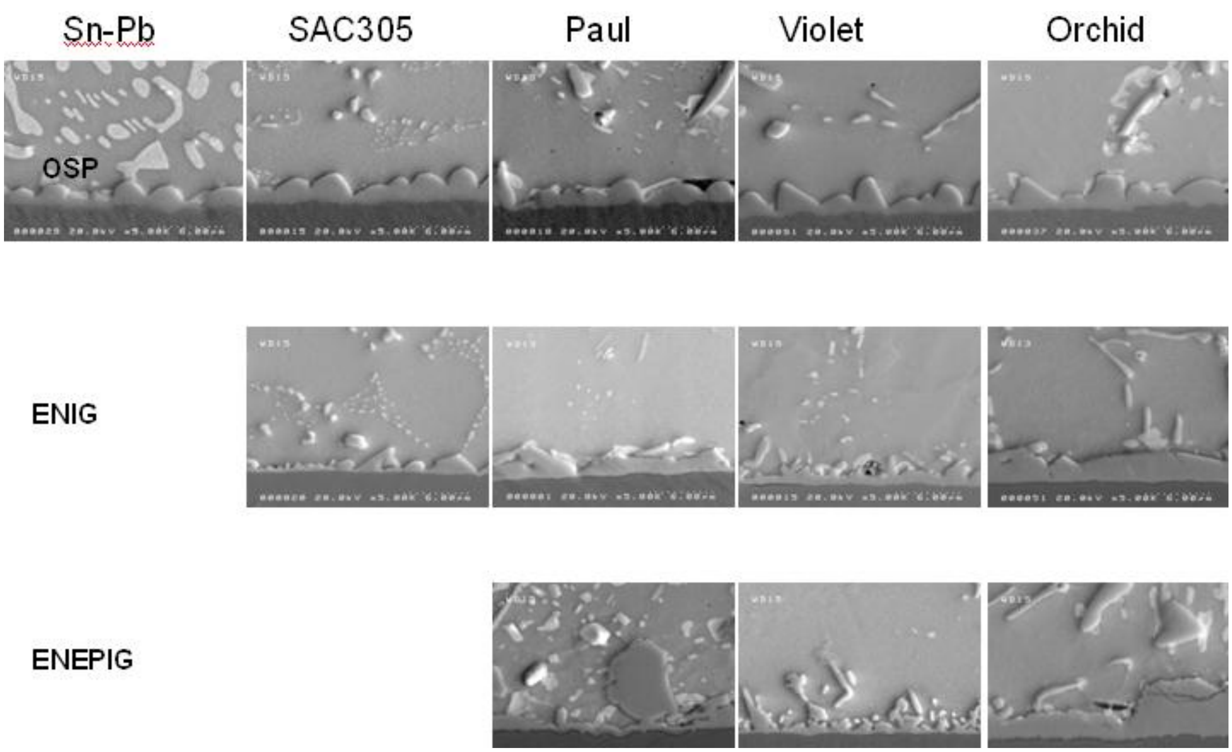

Figure 17: Intermetallic formation in QFP240, SEM, 5000x

Table 14: Intermetallic type

Assembly #	Solder Name	Surface finish	QFP IMC Type		BGA IMC Type	
			Board	Component	Board	Component
1	Tin-Lead	OSP	Cu_6Sn_5	Cu_6Sn_5	$(Cu,Ni)_6Sn_5$	$Cu_{23}Ni_{33}Sn_{44}$
2	SAC305	OSP	Cu_6Sn_5	Cu_6Sn_5	$(Cu,Ni)_6Sn_5$	$Cu_{23}Ni_{33}Sn_{44}$
3	Paul	OSP	Cu_6Sn_5	Cu_6Sn_5	$(Cu,Ni)_6Sn_5$	$Cu_{23}Ni_{33}Sn_{44}$
4	Violet	OSP	Cu_6Sn_5	Cu_6Sn_5	$(Cu,Ni)_6Sn_5$	$Cu_{23}Ni_{33}Sn_{44}$
5	Orchid	OSP	Cu_6Sn_5	Cu_6Sn_5	$(Cu,Ni)_6Sn_5$	$Cu_{23}Ni_{33}Sn_{44}$
6	SAC305	ENIG	$(Cu,Ni)_6Sn_5$	$(Cu,Ni)_6Sn_5$	$Cu_{23}Ni_{33}Sn_{44}$	$Cu_{23}Ni_{33}Sn_{44}$
7	Paul	ENIG	$Cu_{23}Ni_{33}Sn_{44}$	$(Cu,Ni)_6Sn_5$	$(Ni,Cu)_3Sn_4$	$Cu_{23}Ni_{33}Sn_{44}$
8	Violet	ENIG	$Cu_{23}Ni_{33}Sn_{44}$	$(Cu,Ni)_6Sn_5$	$Cu_{23}Ni_{33}Sn_{44}$	$Cu_{23}Ni_{33}Sn_{44}$
9	Orchid	ENIG	$Cu_{23}Ni_{33}Sn_{44}$	$(Cu,Ni)_6Sn_5$	$(Ni,Cu)_3Sn_4$	$Cu_{23}Ni_{33}Sn_{44}$
10	Paul	ENEPIG	$(Cu,Ni,Pd)_6Sn_5$	$(Cu,Ni,Pd)_6Sn_5$	$(Ni,Cu)_3Sn_4+$ $(Pd,Au,Ni,Cu)Sn_4$	$Cu_{23}Ni_{33}Sn_{44}$
11	Violet	ENEPIG	$(Cu,Ni,Pd)_6Sn_5$	$(Cu,Ni,Pd)_6Sn_5$	$Cu_{23}Ni_{33}Sn_{44}$	$Cu_{23}Ni_{33}Sn_{44}$
12	Orchid	ENEPIG	$(Cu,Ni,Pd)_6Sn_5$	$Cu_{23}Ni_{33}Sn_{44}+$ $(Cu,Ni,Pd)_6Sn_5$	$Cu_{23}Ni_{33}Sn_{44}+$ $(Ni,Cu)_3Sn_4+$ $(Pd,Au,Ni,Cu)Sn_4$	$Cu_{23}Ni_{33}Sn_{44}$

The proper interfacial intermetallic layers formation in solder joint is important for harsh environment applications. The intermetallic forms metallurgical bond to common basis materials and, in case of solid thin layer, it has a strengthening effect on solder joints. However, if the interfacial intermetallic layers are thick they can cause joint embitterment. A needle-like irregular intermetallic morphology causing stress concentration may reduce reliability of solder joints. The solder interconnections are different under thermal cycling and drop test conditions. The reliability of electronic products relating to the mechanical properties of intermetallic reaction layers is especially important for harsh environment where the products experience mechanical shock loadings. As the strain-rate increases the stresses in solder interconnections get higher. The intermetallic compound layers will experience significantly higher stresses than those in thermal cycling. Hence, the properties of intermetallic layers, but not those of solder mainly determine the fracture behavior of the interconnections under high strain-rates [15]. The fracture toughness of the joints decreases rapidly with the intermetallic reaction layer thickness increasing. Therefore, the interfacial intermetallic thickness and morphology should be carefully conceded in solder alloy selection.

ATC reliability test results and analysis

ATC results reported below are up to 1548 cycles at -55°C to 125°C. The test is currently ongoing to a 3000 cycle target.

No failures occurred up to 1548 cycles in high Tg (170°C) board material. All three Bi-containing alloys and base line references alloys SAC305 and SnPb assembled on OSP, ENIG and ENEPIG finished boards passed the Airspace qualification requirements of 1000 cycles at -55°C to 125°C.

There were some failures in normal Tg (150°C) board cells. All failures occurred on OSP finished boards. No failures on ENIG and ENEPIG boards were detected. SAC305 assemblies failed before the 1000 cycle criterion. SnPb and Paul alloys passed 1000 cycles at -55°C to 125°C on 150°C Tg boards. Boards assembled using Violet and Orchid did not fail.

The failures isolated to the component location on the 150°C Tg boards are shown in Table 15. These 18 failures were subjected to careful failure analysis. The failed components were cut off the boards and locations of failure were electrically determined. Cross-sections were done through the solder joint and through the related via. The cross-sections of the solder joints and vias are shown in Figures 20 and 21, respectively. The solder joints are absolutely robust.

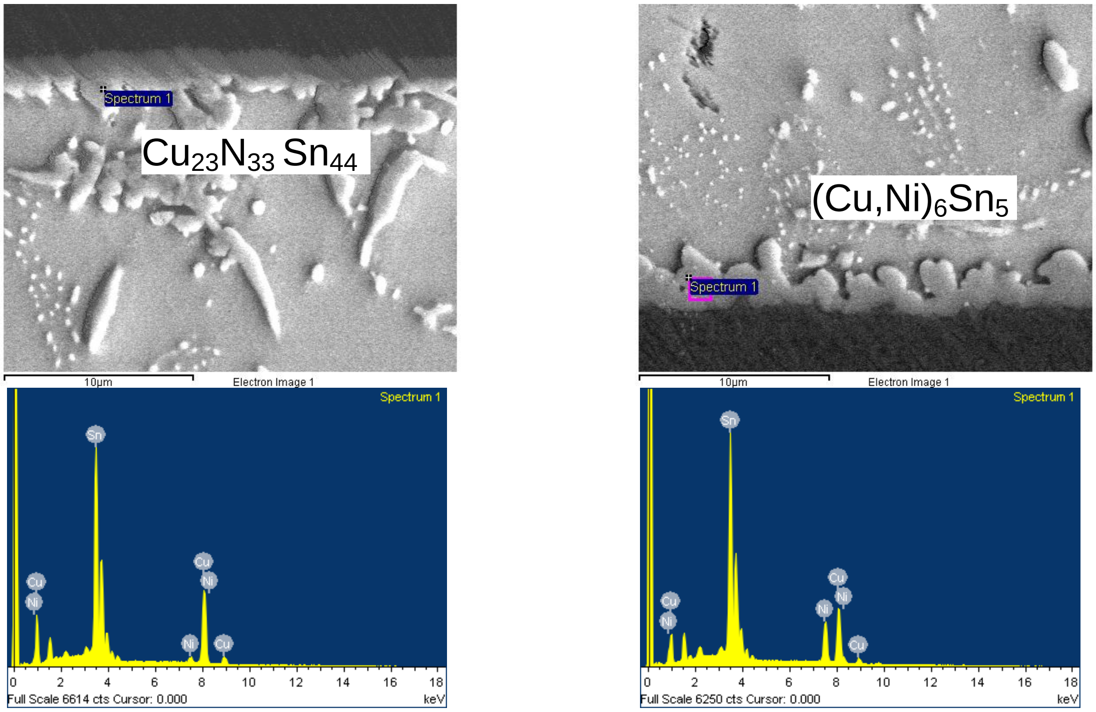

Element	Weight%	Atomic%
Ni K	1.7	2.7
Cu K	36.6	51.2
Sn L	61.7	46.2
Totals	100.0	

a

Element	Weight%	Atomic%
Ni K	13.6	20.1
Cu K	25.8	35.4
Sn L	60.6	44.5
Totals	100.0	

b

Figure 18: EDX analysis of BGA352 solder joint, Paul, OSP: a – board side; b – Component side

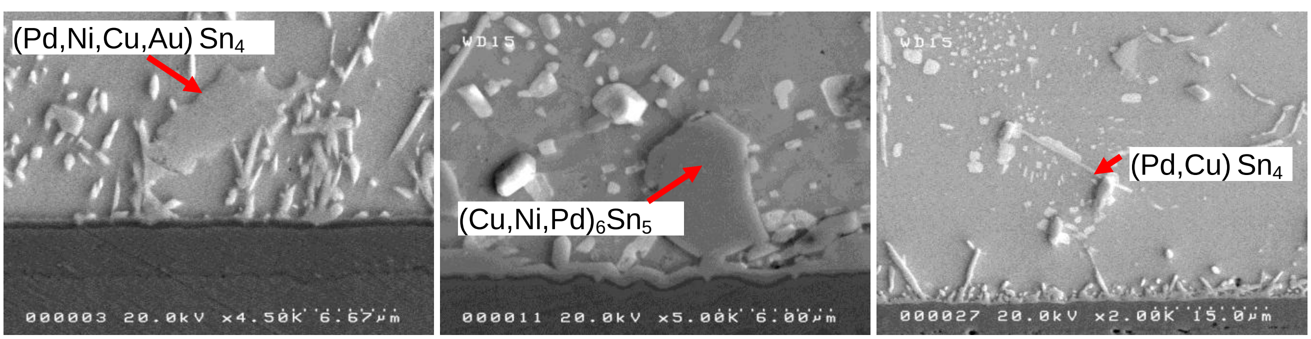

a b c

Figure 19: Pd-containing intermetallics in solder joint, ENEPIG: a - BGA352, Paul; b – QFP240, Orchid; c – BGA352, Violet

Not even micro cracks were found in SSOP48, QFP240, and PLCC84. A tiny micro crack was detected in one of the Paul BGA352 solder joints at the component side. Slightly longer cracks propagate through solder close the component side in the SnPb BGA352. The failures are caused by via failures. The cracks are circular and responsible for open circuits. In the ENIG and ENEPIG cells via cracks are arrested by the Ni barrier layer and do not cause an electrical failure. Early failure of vias in SAC305 cells are attributed to the higher process temperatures that stress the normal Tg board material. The role of the new solder alloy composition in these failures is not fully understood yet. The lack of in vias in cells with the lower Ag content alloys Violet and Orchid might be attributed to their higher compliances and stress absorption in the component locations. ATC is in progress and more work will be done to understand the difference between the alloys.

Table 15: Failure isolated to component locations and confirmed via failures.

Component type	Cycles to failure, -55°C to 125°C	Solder paste	Board finish	Tg
SSOP48	853	SAC305	OSP	150
SSOP48	1072	Paul	OSP	150
SSOP48	1255	Paul	OSP	150
SSOP48	1290	Paul	OSP	150
SSOP48	1256	SnPb	OSP	150
SSOP48	1287	SnPb	OSP	150
QFP240	485	SAC305	OSP	150
QFP240	1062	Paul	OSP	150
QFP240	1275	Paul	OSP	150
QFP240	1287	Paul	OSP	150
PLCC84	1005	Paul	OSP	150
PLCC84	1464	Paul	OSP	150
PLCC84	1504	Paul	OSP	150
352BGA	504	SAC305	OSP	150
352BGA	598	SAC305	OSP	150
352BGA	1043	Paul	OSP	150
352BGA	1067	Paul	OSP	150
352BGA	1341	SnPb	OSP	150

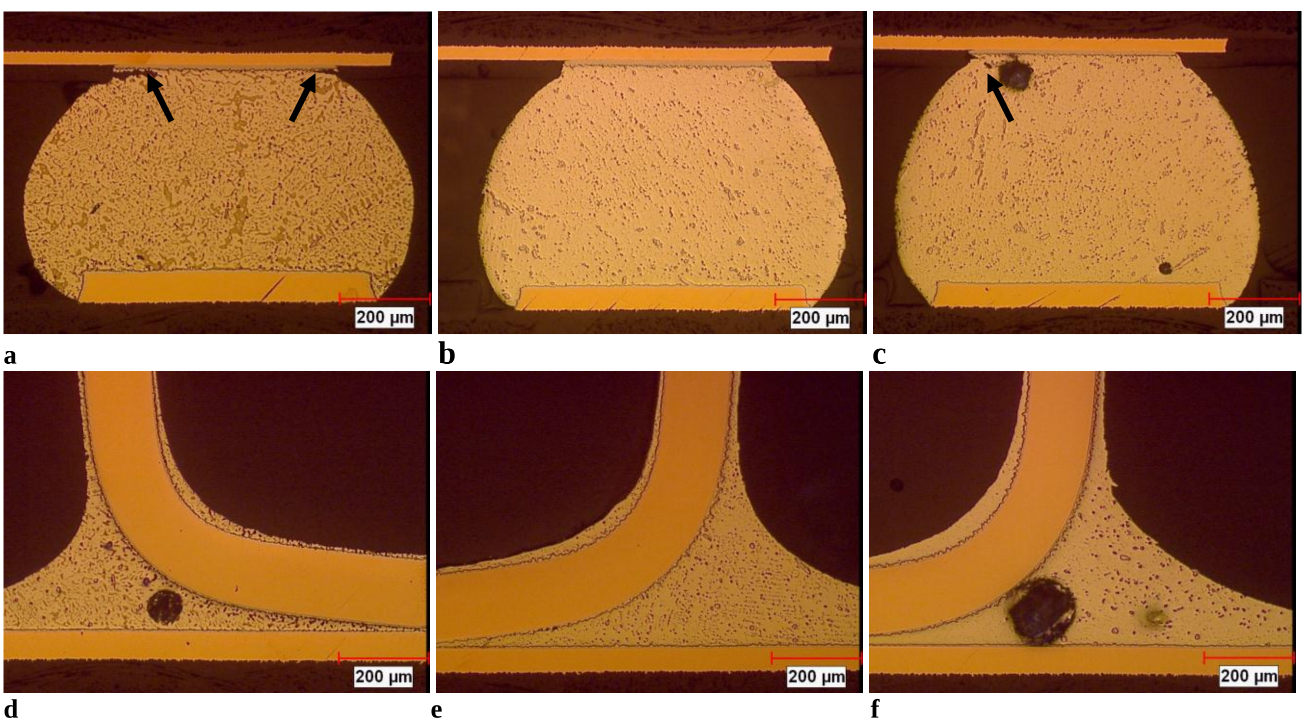

Figure 20: Microstructure of solder joints formed on 150°C Tg boards with OSP finish after -55°C to 125°C cycling: a – BGA351, Sn-Pb, 1257 cycles; b - BGA352, Paul, 1067 cycles; c – BGA352, Paul, 1043 cycles; d - SSOP48, SnPb, 1257 cycles; e - SSOP48, Paul, 1255 cycles; e - SSOP48SAC305, 853 cycles

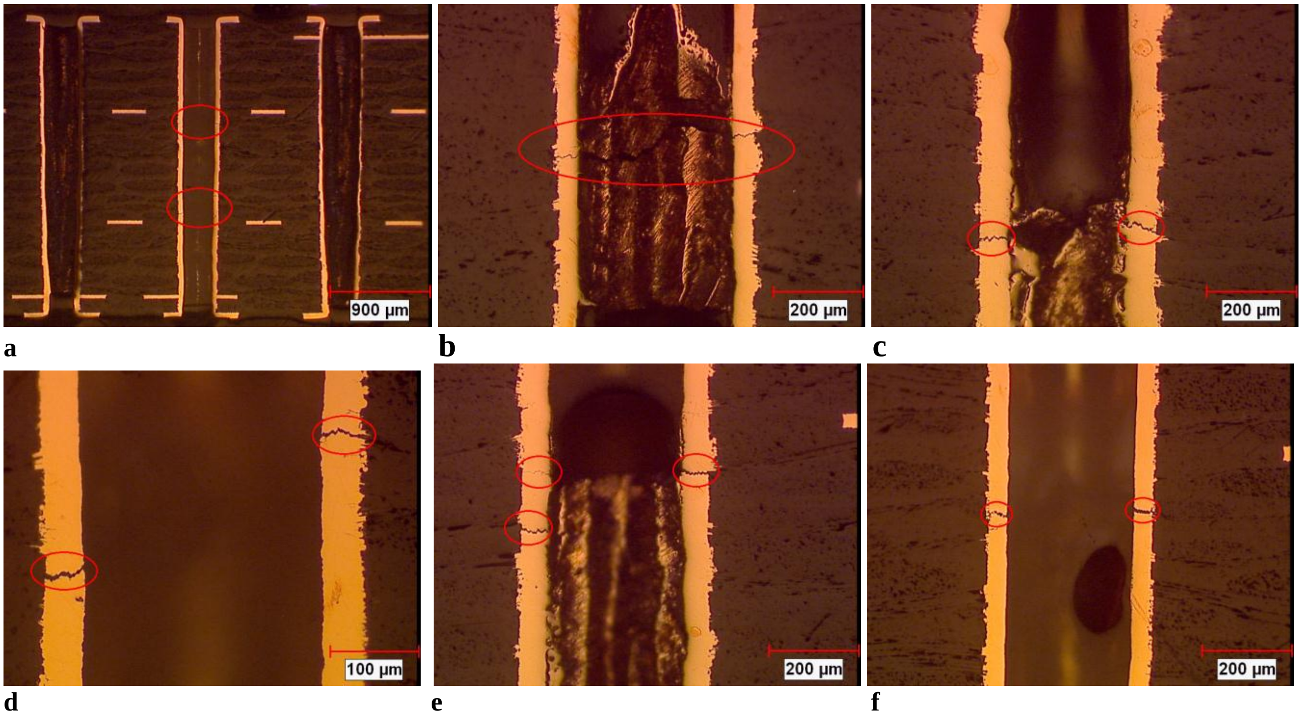

Figure 21: Broken vias on 150°C TG boards with OSP finish after -55°C to 125°C cycling: a – Typical location; b – Circular shape; c - BGA352, Paul, 1067 cycles; d - Paul, 1067 cycles; e - C305, 853 cycles, 1255 cycles; e - Sn-Pb, 1257 cycles

Vibration test results and analysis

Vibration testing is ongoing and will be discussed in the follow up paper.

Summary and Conclusions

Screening experiments on the manufacturability and reliability of the lower melting Pb-free alloys that may satisfy the Aerospace requirements are in progress. The following results and conclusions may be made at this time.

Three Bi-containing alloys: Sn3.4Ag4.8Bi (Paul) and two reduced Ag content variations, with and without Cu, Sn2.25Ag0.5Cu6Bi (Violet) and Sn2Ag 7Bi (Orchid), were selected. Honeywell test vehicles were assembled using these alloys with the process temperature about 10°C below than SAC305. Two board materials with high Tg and normal Tg were used. The boards were finished with OSP, ENIG, and ENEPIG. No problems related to the manufacturability were detected. Experimental alloys had better wetting and less voiding than SAC305. The joints had a proper shape comparable to both SnPb and SAC305.

The microstructural analysis after assembly revealed that

- All three Bi-containing alloys formed excellent joints on OSP finish. The interfacial intermetallic layer is comparable to SnPb in thickness and shape and thinner than in SAC305
- Sn3.4Ag4.8Bi (Paul) and Sn2Ag 7Bi (Orchid) are not fully compatible with ENIG and ENEPIG, forming irregular and/or thicker interfacial intermetallic than SAC305. This is attributed to the lack of Cu in these alloy compositions.
- The alloy with Cu, Sn2.25Ag0.5Cu6Bi (Violet), is compatible not only with OSP, but also with ENIG and ENEPIG, and forms excellent solder joints with uniform intermetallic layers on both ball grid array and leaded components
- On the ENEPIG finish, Pd-containing needle-shaped intermetallic particles are present in solder joints. These particles may cause solder joint embrittlement. The ENEPIG finish must be fully qualified for Aerospace industry acceptance.

There was no solder joint failure on both high and normal Tg boards after 1548 cycles at -55°C to 125°C completion. However, there were via failures in normal Tg boards with OSP finish, assembled using SAC305, Sn3.4Ag4.8Bi (Paul), and SnPb solders. Of these via failures on normal Tg OSP finished boards only the SAC305 cell did not meet the Aerospace qualification requirement of 1000cycles. Therefore, all three experimental alloys Paul, Violet, and Orchid showed excellent performance in harsh environment thermal cycling.

Further ATC and vibration testing are in progress. More results will be reported upon the program completion.

Future work

As the tests are still in progress, the next paper will focus on the results and analysis of ATC 3000 cycles and the vibration testing. Additional cross-section analysis of the solder joints after completion of 3000 cycles will also be performed and presented in the next paper. Finally a discussion of the alloy performance for ATC and vibration as well as additional analysis on the alloy metallurgical properties will be published

Discussions are under way to share these results to help launch a new NASA consortium phase 3 project focused on the requirements of the Aerospace industry. These screening test results will be shared and used to take the next steps in the lower melt alloy development.

Acknowledgements

The authors would like to thank the following individuals from Celestica: Russell Brush, Alon Walk, Kangwon Lee, Veseyathaas Thambipillai for ATC testing and data analysis; Jie Qian for sample preparation; Jose Traya and Michael Emery for test vehicle assembly; Suthakaran Subramaniam and Michelle Le for vibration testing; and Dr. John Vic Grice Honeywell Corporate consulting statistician who helped design the experimental matrix.

References

[1] http://www.teerm.nasa.gov/nasa_dodleadfreeelectronics_proj2.htm.

[2] "Properties of Ternary Sn-Ag-Bi Solder Alloys: Part 1- Thermal properties and microstructure Analysis", P. Vianco, et al.. Journal of Electronics Materials, Vol.28, No.10, pp. 1127-1137, 1999.

[3] "Properties of Ternary Sn-Ag-Bi Solder Alloys: Part 2- Wettability and Mechanical properties Analysis", P. Vianco, et al.. Journal of Electronics Materials, Vol.28, No.10, pp. 1138-1143, 1999.

[4] "Creep Behavior of Bi-Containing Lea-Free Solder Alloys", D. Witkin, et al.. Journal of Electronics Materials, Vol.41, No.2, pp. 190-203, 2012.

[5] "Lead-Free Electronics: iNEMI Projects Lead to Successful Manufacturing", E. Bradley, C. A. Handwerker, J. Bath, R. D. Parker, R. W. Gedney , 472 pages, 2007.

[6] http://www.freesamplesite.com/ydf/showthread.php/149076-Free-NCMS-Lead-Free-Solder-Project-CD-Rom NSMS, Lead-Free, High-Temperature, Fatigue-Resistant Solder: Final Report , Ann Arbor, MI: National Center for Manufacturing Science, 2001.

[7] http://www.aciusa.org/leadfree/LFS.../02_GREENE_JG-PP_JCAA_Program.pdf.

[8] "Conception and Production of high reliable PWB-assemblies for thermally and mechanically highly stressed long term reliable lead free electronic systems for Aeronautics" Dr. Ing. G. Reichelt. German Joint Project. Perm # 8, Noordwijk, 2011.

[9] "New generation of Lead-free Solder Alloys: Possible Solution to Solve Current Issues with Main Stream Lead-free Soldering", P. Snugovsky, S. Bagheri, M. Romansky, Celestica Inc. Toronto, D. Perovic, L. Snugovsky, J. Rutter, University of Toronto. SMTA Journal, Vol. 25 Issue 3, 2012.

[10] "Assembly Feasibility and Property Evaluation of New Low Melt Solder Alloys", E. Kosiba, et al., ICSR SMTA proceedings, Toronto. 2012.

[11] "Design and Analysis of Experiments", Montgomery, D.C., "7th edition. John Wiley & Sons, 2009.

[12] "Lead-free solder systems: phase relations and microstructures", P. J. T. L. Oberndorff. PhD Thesis, Techische Universiteit Eindhoven, the Netherlands, 2001.

[13] "Phase Equilibria in the Sn-rich Corner of the Cu-Ni-Sn System", L. Snugovsky, P. Snugovsky, D.D. Perovic and J.W. Rutter. Materials Science and Technology, vol. 29, No 8, pp. 899 – 902, 2006.

[14] "Interfacial reaction issues for lead-free electronic solders", C. E. Ho, S. C. Yang, C. R. Kao. Journal of Materials Science, 18:155–174 DOI 10.1007/s10854-006-9031-5 123, 2007.

[15] “Effect of Solid-state Intermetallic Growth on the Fracture Toughness of Cu/63Sn-37Pb Solder Joints”, Ronald E. Pratt, Eric I. Stromswold, and D. J. Quesnel. IEEE Transactions on Components, Packaging, and Manufacturing Technology-Part A, vol. 19, No. 1, Mar. 1996.

Manufacturability and Reliability Screening of Lower Melting Point Pb-Free Alloys Containing Bi

Celestica, Inc.
Toronto, Canada

Polina Snugovsky,
Eva Kosiba, Jeffrey Kennedy,
Zohreh Bagheri,
Marianne Romansky,

polina@celestica.com

Honeywell
Arizona, USA

Michael Robinson,
Joseph M. Juarez, Jr.,
Joel Heebink

mike.robinson6@honeywell.com
joseph.juarez@honeywell.com

Problem Statement

- Aerospace and defense organizations exercise RoHS exemptions and research reliability for RoHS compliant solders
- Aerospace and Military products need better
  - vibration performance
  - drop/shock performance
  - combined environment reliability

  than RoHS SAC305 alloy
- Pad cratering is a dominant failure mode especially under dynamic loading

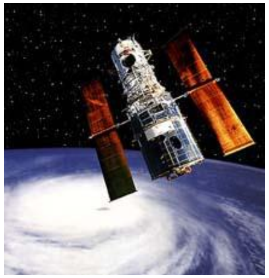

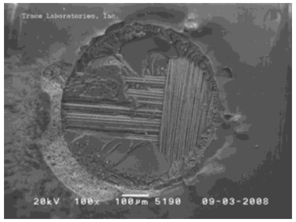

Possible Solution

- Pb-free solders with lower process temperatures
  - Reduces thermal damage to boards and components
  - Lower Tg board materials are less prone to pad cratering defects
- Several Sn-Ag-Bi and Sn-Ag-Cu-Bi alloys are available
  - Melt about 10° C lower than SAC305.
  - Bismuth
    - Reduces melting temperature
    - Improves thermomechanical behavior
    - Reduces propensity to whisker growth
    - Not used due to Sn-Pb-Bi low melting ternary eutectic (96° C) and peritectic (137° C)

Time to use Bi containing alloys.

Pb has been removed from component finishes

Background

- Celestica Pb-free lower melt alloy program began in 2009
- Objective:
  - Select new Pb-free solder alloys with process temperatures comparable to conventional SnPb solder for assembly and rework of all component types

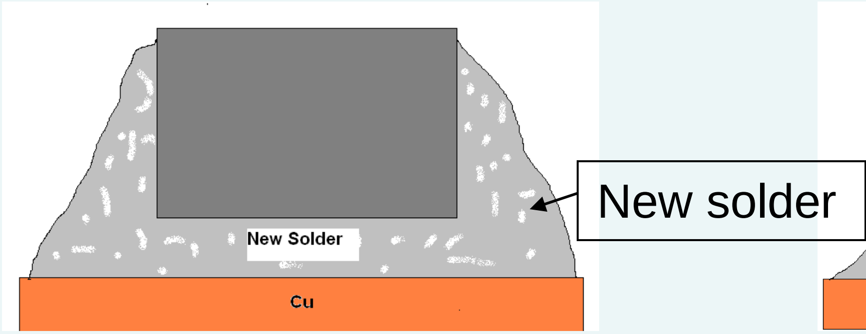

1. Leaded and discrete components

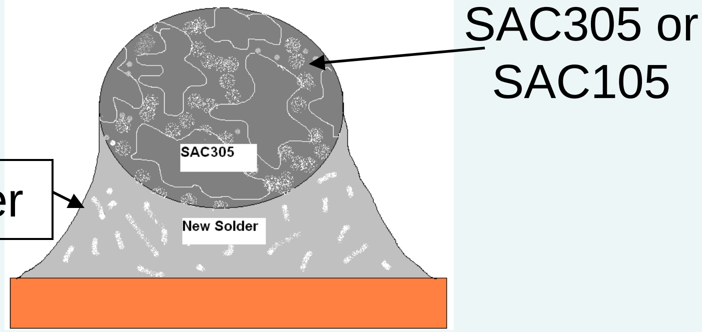

2. Ball grid alloy components

  - Use of standard laminate materials
  - Low Ag or no Ag alloys cheaper and more compliant
  - Interconnects with improved mechanical and thermal mechanical performance

Benefits

1. Low melting temperature
    - Reduce process temperature
    - Use cheaper board – material - normal Tg
    - Mitigate pad cratering
    - Reduce de-lamination and cracking caused by entrapped moisture
    - Reduce warpage
    - Reduce Pad-in-Pillow
    - Eliminate baking
    - Use temperature sensitive components

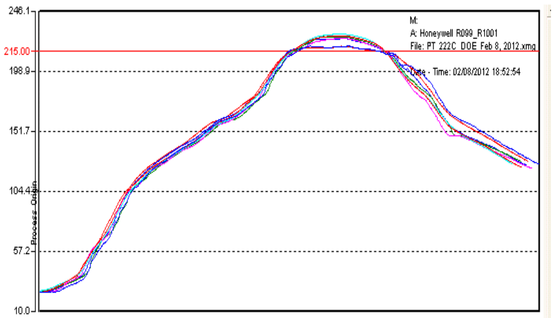

2. No or low Ag
    - Prevent Ag_3Sn platelets formation
    - Better mechanical properties - reduced toughness
    - Cheaper than SAC 305
    - More environmentally friendly
3. 3. Bi in composition
    - Better mechanical properties – better performance under vibration
    - *Reduce whisker propensity*
4. 4. Cu and Bi in composition together with lower process temperature
    - Cu dissolution should not be such a problem

Results to Date

- Phase 1: Alloys selection, Celestica & U of T – 2009
  - Requirements formulation
  - Literature and phase diagrams analysis
  - Sample preparation: alloys, joints on Cu, BGA
  - Metallurgical analysis: microstructure and DSC
  - Ranking and recommendation for future work
- Phase 2: Manufacturing feasibility, Celestica – 2010
  - Solder paste evaluation
  - Reflow and rework profile selection
  - Test vehicle assembly and analysis
  - 7 alloys recommended for future work
- Phase 3: Screening experiments, Celestica & Customers – 2011-2013
  - Consumer electronics
  - Telecommunications
  - Aerospace

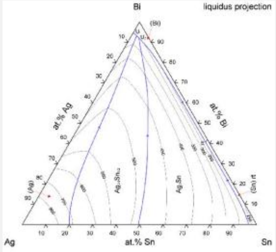

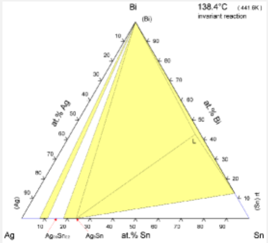

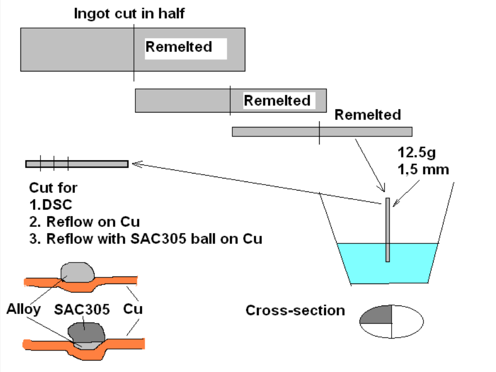

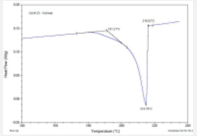

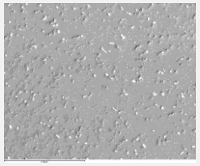

Celestica/Honeywell
Lower Melt Alloy Program

- Explores the manufacturability and reliability for the Bi-containing alloys in comparison to conventional SAC305 and SnPb assemblies
  - Alloy selection
  - Test vehicle
  - Assembly
  - Accelerated temperature cycling
  - Vibration testing plan
  - As assembled solder joint quality and microstructure
  - ATC reliability test results and analysis
  - Summary and conclusions
  - Future work

Alloy Selected for High Reliability Screening Experiments

#	Celestica Name	Alloy constituents	Alloy composition	Min Melting Temperatures, ° C (Experimental)	Melting Range, ° C
1	Paul	SnAgBi	Sn3.4%Ag4.8%Bi	206	11
2	Violet	SnAgCuBi	Sn2.25%Ag0.5%Cu6.0%Bi	205	10
3	Orchid	SnAgBi	Sn2.0%Ag7.0%Bi	190	25
4	SAC305	SnAgCu	Sn3.0%Ag0.5%Cu	217	6
5	Eutectic SnPb	SnPb	Sn37.0%Pb	183	0

Alloy Selection

- #1 “Paul” **Sn3.4%Ag4.8%Bi** was proposed by Paul Vianco
  - Excellent pasty range
  - Excellent thermomechanical properties for harsh environments
    - proved by NCMS and the German Joint Lead-Free Avionics project
- #2 “Violet” **Sn2.25%Ag0.5%Cu6.0%Bi** is a variant of “Paul”
  - Excellent pasty range
  - Lower Ag content, does not form Ag_3Sn plates
    - may help to improve drop/shock properties
  - Cu to reduce the Cu dissolution potential
  - Higher Bi related to reduced Ag may help to better mitigate whisker formation
- #3 “Orchid” **Sn2.0%Ag7.0%Bi** is a variant of the “Paul”
  - Pasty range is wider than in alloys #1 and #2
  - lower Ag and higher Bi
    - reduction of the minimum melting temperature.
  - may show greater whisker mitigation
- SAC305 and Sn-Pb solders were included in the test matrix for comparison.

Test Vehicle

- Honeywell designed
- Used for numerous Sn-Pb baseline and Pb-free process development
- Board stack-up and dimensions are representative of a large percentage of aerospace products
- Designed per IPC-4101/126 & /129 requirements

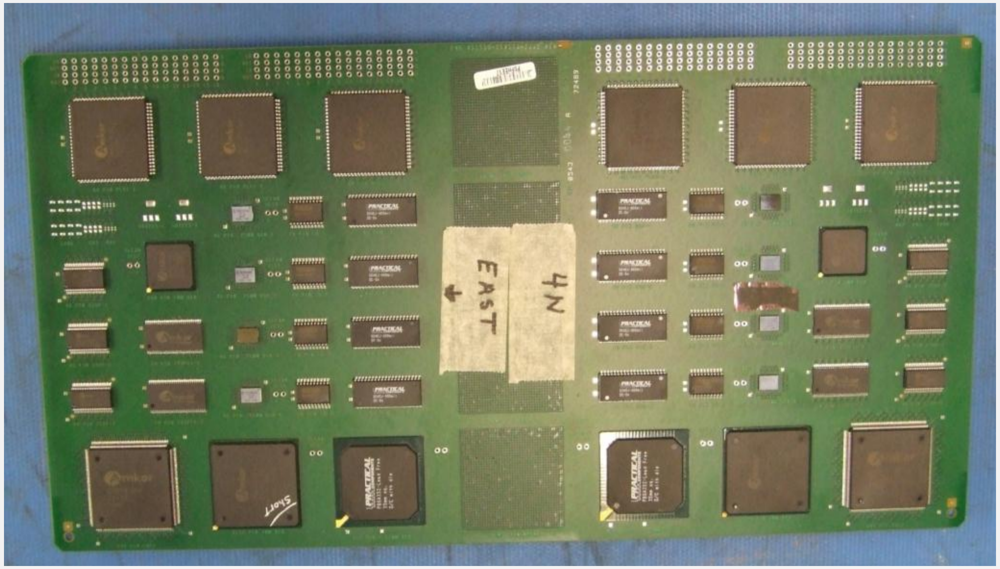

- 203mm x 355mm and 2.5mm
- 16 layers of alternating signal and ground/power plane with copper
- Daisy chained

Solder paste

- No-clean solder pastes of the experimental alloys were produced by one of the major solder paste suppliers
- Solder paste performance evaluation was done using a standard Celestica solder paste evaluation procedure

Laminate materials

Tg (°C)	LAMINATE	SUPPLIER
150	Nelco 4000-7	Holaday Circuits
170	Isola 370HR	Holaday Circuits

Surface finishes

SURFACE FINISH	THICKNESS (µm)
OSP	Entek 106A (Copper Triazole)
ENIG	MacDermid Ni 3.81µm - 0.13-0.20µm Au
ENEPIG	Uyemura Ni 3.81µm – 0.05µm Pd – 0.08µm Au

Component types

I/O COUNT/ PACKAGE	DIMENSIONS, mm	PITCH, mm	LEAD FINISH	BALL COMPOSITION
20 SO	6.35 X 12.70	1.27	Sn-Pb and Sn	
40 SOJ	10.16 X 25.40	1.27	Sn-Pb and Sn	
48 SOP	5.08 X 15.24	0.50	Sn-Pb and Sn	
54 TSSOP	10.16 X 21.59	0.64	Sn-Pb and Sn	
84 PLCC	29.21 X 29.21	1.27	Sn-Pb and Sn	
240 PQFP	31.75 X 31.75	0.50	Sn-Pb and Sn	
289 BGA	17.15 X 17.15	1.02		SAC 305
352 BGA	35.56 X 35.56	1.27		SAC 305
1156 BGA	34.93 X 34.93	1.02		SAC 305

Statistical Considerations

Experimental Design using Three Factors Applied to the Failure of Six Components Using a Latin Square for Run Combinations 1-9 and a Full Factorial for Runs 10-17

Paste type Finish T_g	Paul			Violet			Orchid			SAC305				Sn-Pb			
	OSP	ENIG	ENEPIG	OSP	ENIG	ENEPIG	OSP	ENIG	ENEPIG	OSP	OSP	ENEPIG	ENEPIG	OSP	OSP	ENEPIG	ENEPIG
	150	170	170	170	150	170	170	170	150	150	170	150	170	150	170	150	170
Component Type	1	2	3	4	5	6	7	8	9	10	11	12	13	14	15	16	17
352 BGA	/02	/02	/02	/02	/02	/02	/02	/02	/02	/02	/02	/02	/02	/02	/02	/02	/02
240 QFP	/02	/02	/02	/02	/02	/02	/02	/02	/02	/02	/02	/02	/02	/02	/02	/02	/02
SSOP 48	/06	/06	/06	/06	/06	/06	/06	/06	/06	/06	/06	/06	/06	/06	/06	/06	/06
PLCC 84	/06	/06	/06	/06	/06	/06	/06	/06	/06	/06	/06	/06	/06	/06	/06	/06	/06
SO 20	/08	/08	/08	/08	/08	/08	/08	/08	/08	/08	/08	/08	/08	/08	/08	/08	/08
SOJ 40	/08	/08	/08	/08	/08	/08	/08	/08	/08	/08	/08	/08	/08	/08	/08	/08	/08

Latin Square of Paste and Finish

PASTE	Finish		
	OSP	ENIG	ENEPIG
Paul	150	170	170
Violet	170	150	170
Orchid	170	170	150

Assembly

- 56 test vehicles built at Celestica
- 7 thermocouples placed on the board
- Reflowed in a 10-zone Electovert Omniflow oven
- Siemens Siplace X3 SMT placement machine
- Visual and Xray

Build Matrix

BOARD MATERIAL	ALLOY	SURFACE FINISH		
		ENEPIG	ENIG	OSP
Normal Tg	SnPb	2		3
	SAC305	2		2
	Paul			4
	Violet		4	
	Orchid	4		
High Tg	SnPb	2		3
	SAC305	2	1	3
	Paul	4	4	
	Violet	4		4
	Orchid		4	4

Reflow Profile for 222°C

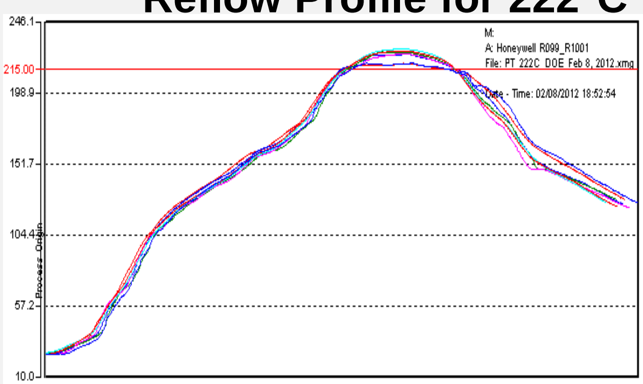

Reflow Profile for 240°C

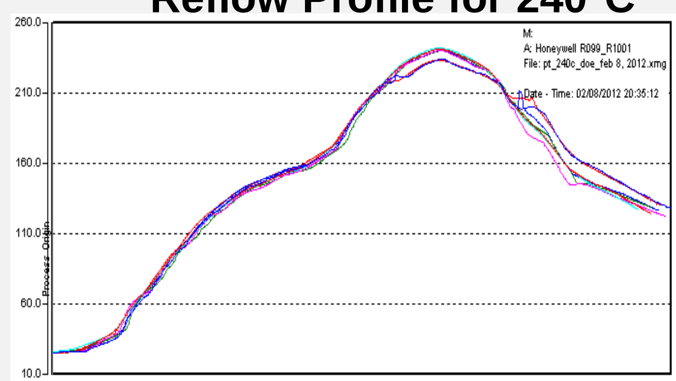

As Assembled Solder Joint Quality

- Acceptable solder joints in all assemblies
  - Voiding
  - Wetting
  - Shape and size
- No major anomalies or concerns
- Experimental alloys have less voiding than SAC305 and comparable to SnPb
- The lower level of voiding on ENEPIG followed by ENIG and then OSP
- Wetting on OSP is improved for the experimental alloys containing Bi

Voiding in BGA352

##	Solder Name	Surface	Voiding,%
1	Tin-Lead	OSP	15.7
2	SAC305	OSP	24.5
3	Paul	OSP	17.7
4	Violet	OSP	22.0
5	Orchid	OSP	17.2
6	SAC305	ENIG	23.2
7	Paul	ENIG	13.0
8	Violet	ENIG	12.1
9	Orchid	ENIG	12.9
10	Paul	ENEPIG	10.5
11	Violet	ENEPIG	3.5
12	Orchid	ENEPIG	10.7

SnPb SAC305 Paul Violet Orchid

As Assembled Solder Joint Microstructure

- Cross-sections and microstructure analysis were done on
  - BGA352 location U200 exposed to the lowest temperature during reflow
    - the center - 224.9° C, the corner balls - 227.5° C
    - cross-sectioned diagonally
  - QFP240 location U23 experienced the hottest temperature - 232° C

BGA352

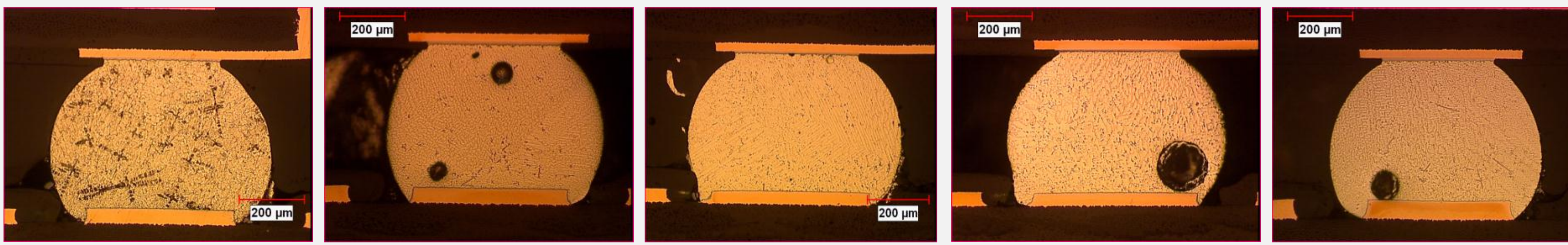

QFP240

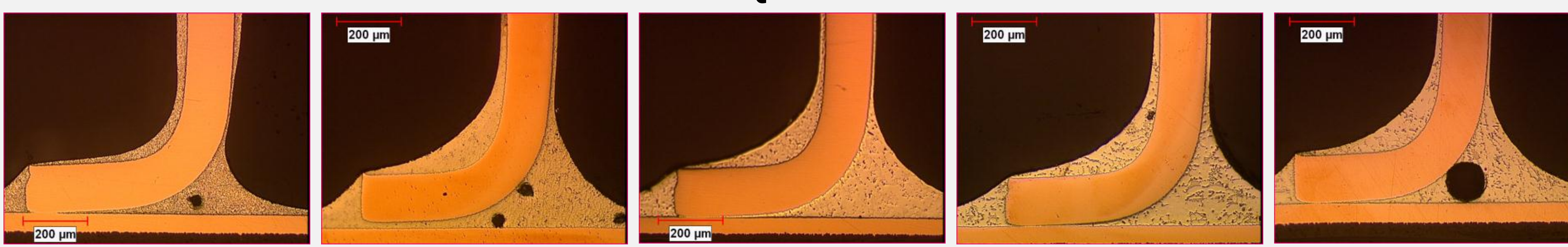

SnPb **SAC305** **Paul** **Violet** **Orchid**

BGA352 Joint Composition After Assembly

- SAC305 solder balls completely mixed with solders
- Lower Ag in Violet and Orchid
- Cu dissolves in solder joints formed on OSP boards
  - SnPb joints contain 0.4%Cu
  - The Cu content in Pb-free joints on OSP boards is 2X higher than on ENIG and ENEPIG

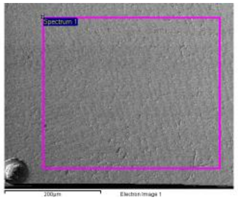

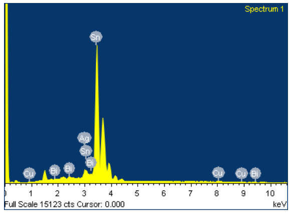

##	Solder Name	Surface finish	BGA Composition				
			Sn	Ag	Cu	Bi	Pb
1	Tin-Lead	OSP	70.2	0	0.4	0	29.4
2	SAC305	OSP	96.2	2.8	1.0	0	0
3	Paul	OSP	95.0	2.6	0.8	1.7	0
4	Violet	OSP	95.7	2.1	0.7	1.5	0
5	Orchid	OSP	94.7	2.3	1.0	2.0	0
6	SAC305	ENIG	96.7	2.8	0.5	0	0
7	Paul	ENIG	95.9	3.0	0.3	0.8	0
8	Violet	ENIG	95.5	2.2	0.6	1.7	0
9	Orchid	ENIG	95.0	2.5	0.4	2.1	0
10	Paul	ENEPIG	95.0	2.5	0.4	2.1	0
11	Violet	ENEPIG	95.1	2.8	0.6	1.5	0
12	Orchid	ENEPIG	95.5	2.2	0.4	1.9	0

Bi Content in Sn Grains

# #	Solder Name	Surface finish	QFP		BGA	
			Wt %	At %	Wt %	At %
1	Tin-Lead	OSP	0	0	0	0
2	SAC305	OSP	0	0	0	0
3	Paul	OSP	3.1	1.8	1.5	0.9
4	Violet	OSP	3.8	2.2	1.4	0.8
5	Orchid	OSP	3.8	2.2	2.1	1.2
6	SAC305	ENIG	0	0	0	0
7	Paul	ENIG	3.8	2.2	1.2	0.7
8	Violet	ENIG	3.7	2.1	1.9	1.1
9	Orchid	ENIG	4.1	2.4	2.4	1.4
10	Paul	ENEPIG	4.0	2.3	2.0	1.1
11	Violet	ENEPIG	3.5	2.0	2.0	1.1
12	Orchid	ENEPIG	3.5	2.0	1.6	0.9

Bi Content in Sn Grains

BGA352:
- About 2 wt% (1at %) – close to solubility in Sn at ambient condition
- Solid-solution strengthening
- Bi precipitation not expected

QFP240:
- 3 to 4 wt% Bi - 2X higher than Bi dissolution limit at room temperature
- Bi is expected to precipitate in Sn matrix
- Solid-solution and precipitation strengthening

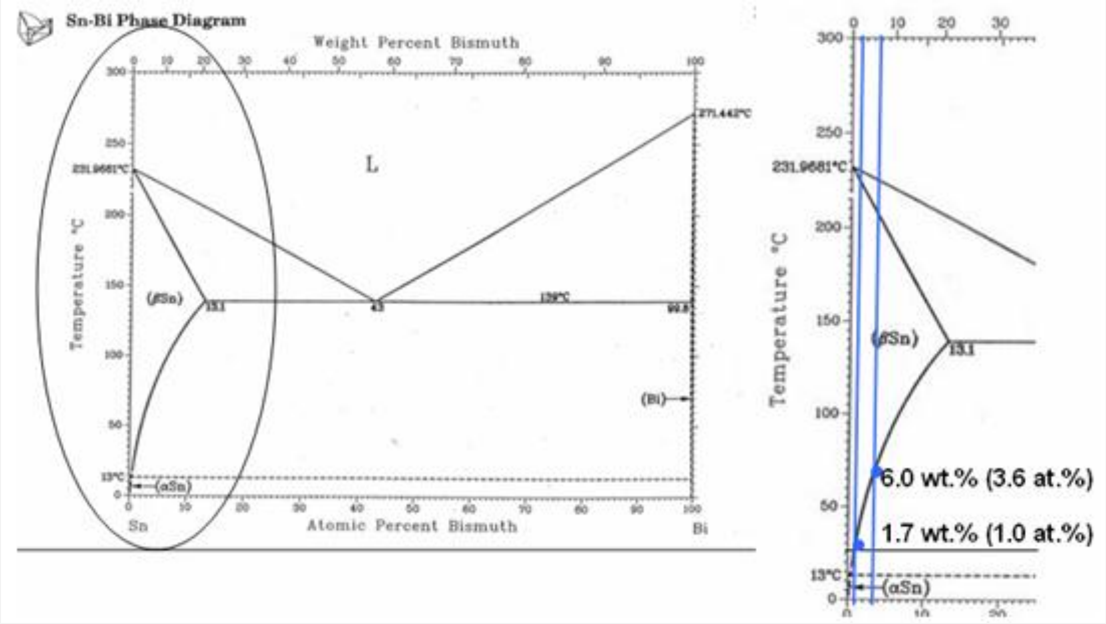

As Assembled BGA352 Microstructure

- The experimental alloys microstructure is similar to SAC305
  - primary-like Sn dendrites and interdendritic eutectic: Ag_3Sn + Sn or Ag_3Sn + Cu_6Sn_5 + Sn
- The diameter of Sn dendrite branches is smaller in SAC305 than in Bi containing alloys
- The dendritic structure in OSP joints is finer than in ENIG and ENEPIG joints
- No Bi precipitation in BGA352

OSP

ENEPIG

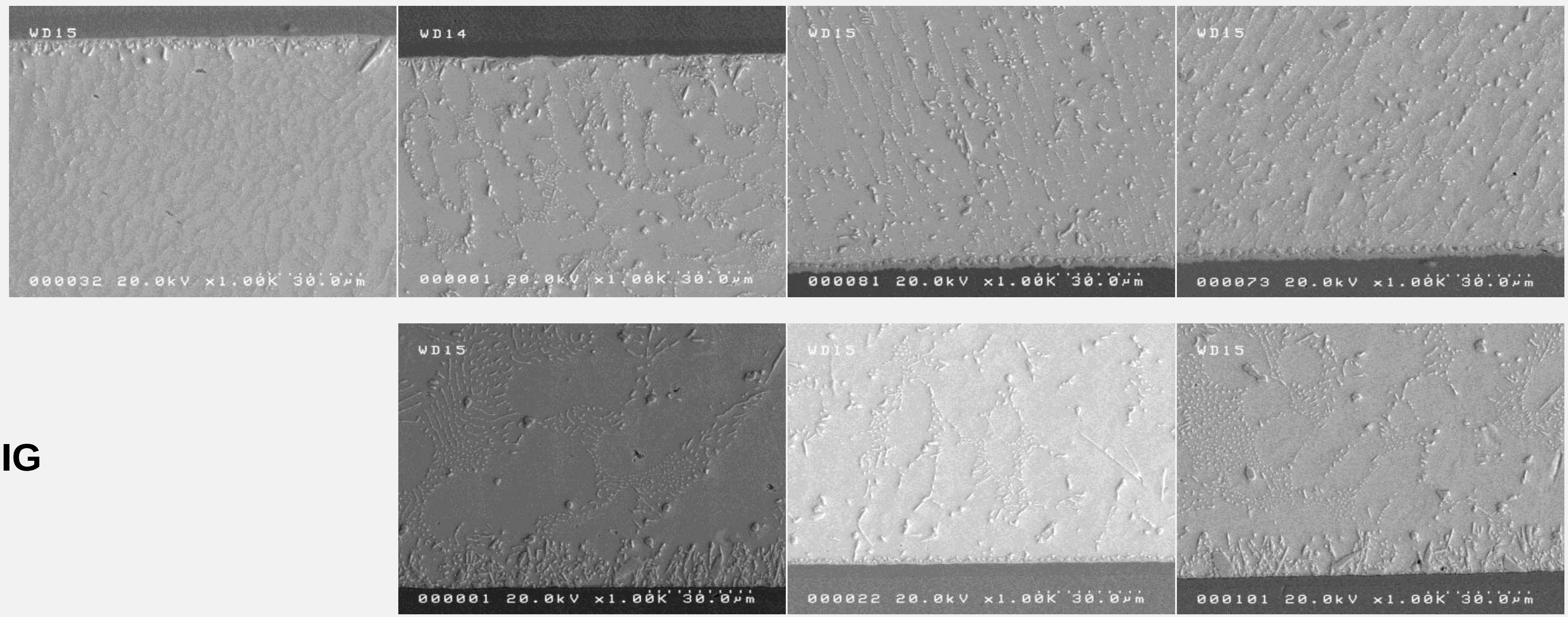

SnPb **Paul** **Violet** **Orchid**

As Assembled QFP240 Microstructure

- Primary-like Sn dendrites and eutectic: Ag_3Sn + Sn or Ag_3Sn + Cu_6Sn_5 + Sn
- Bi particles in the eutectic regions and inside the primary Sn grains
- The dendritic structure of the experimental alloys is coarser than in SAC305

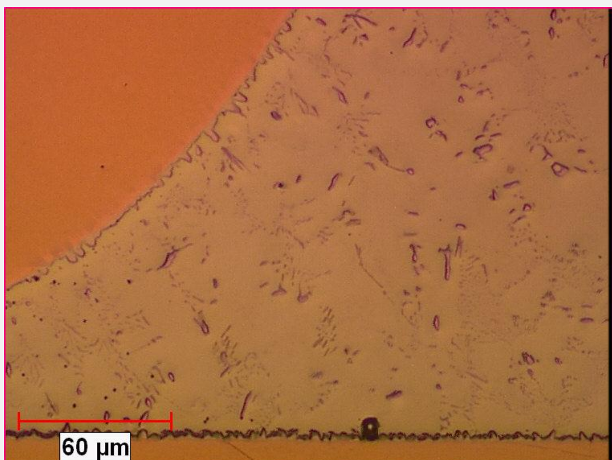

Paul, OSP

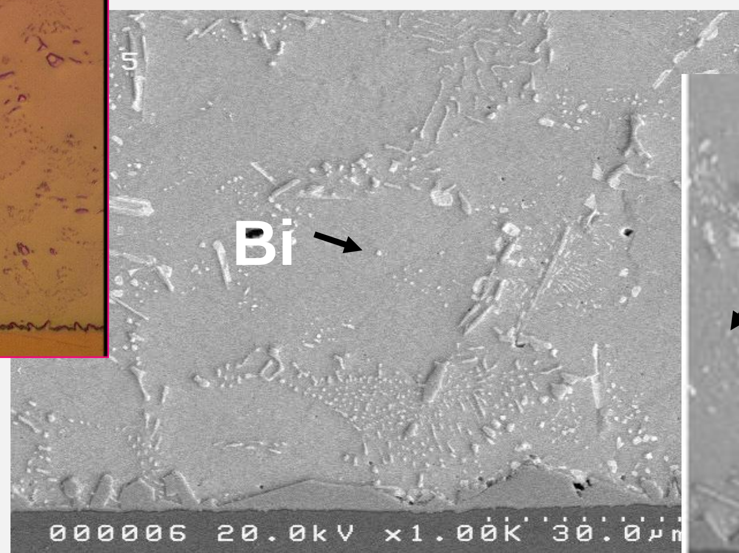

Violet, ENEPIG

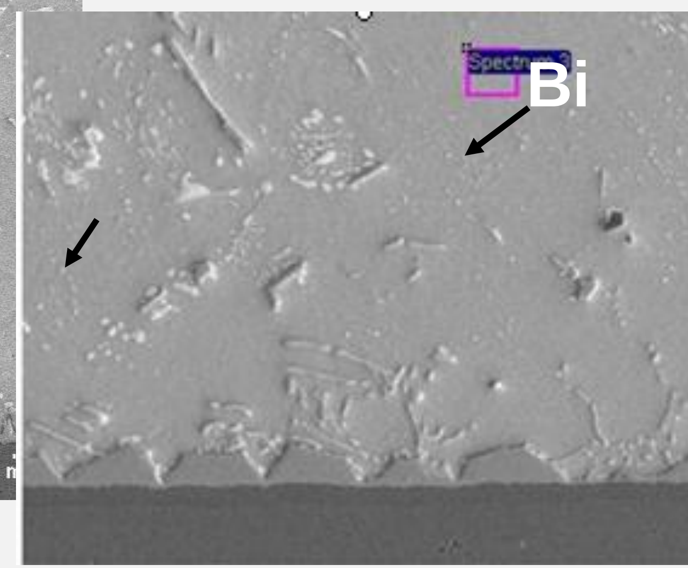

Orchid, ENEPIG

Intermetallic Thickness

# #	Solder Name	Surface Finish	QFP IMC Thickness, µm		BGA, IMC Thickness, µm	
			Board	Component	Board	Component
1	Tin-Lead	OSP	1.8	2.0	2.2	2.1
2	SAC305	OSP	2.1	2.5	3.3	2.4
3	Paul	OSP	1.9	1.9	2.4	1.5
4	Violet	OSP	1.9	2.2	2.1	1.7
5	Orchid	OSP	2.0	2.2	2.4	1.6
6	SAC305	ENIG	1.2	2.3	1.6	1.4
7	Paul	ENIG	2.1	3.6	1.0	1.3
8	Violet	ENIG	1.7	2.6	2.1	1.2
9	Orchid	ENIG	2.9	3.5	1.9	1.5
10	Paul	ENEPIG	1.5	3.5	Irregular	1.7
11	Violet	ENEPIG	1.8	2.1	1.1	0.9
12	Orchid	ENEPIG	3.9	3.2	Irregular	1.6

BGA352: IMC Morphology

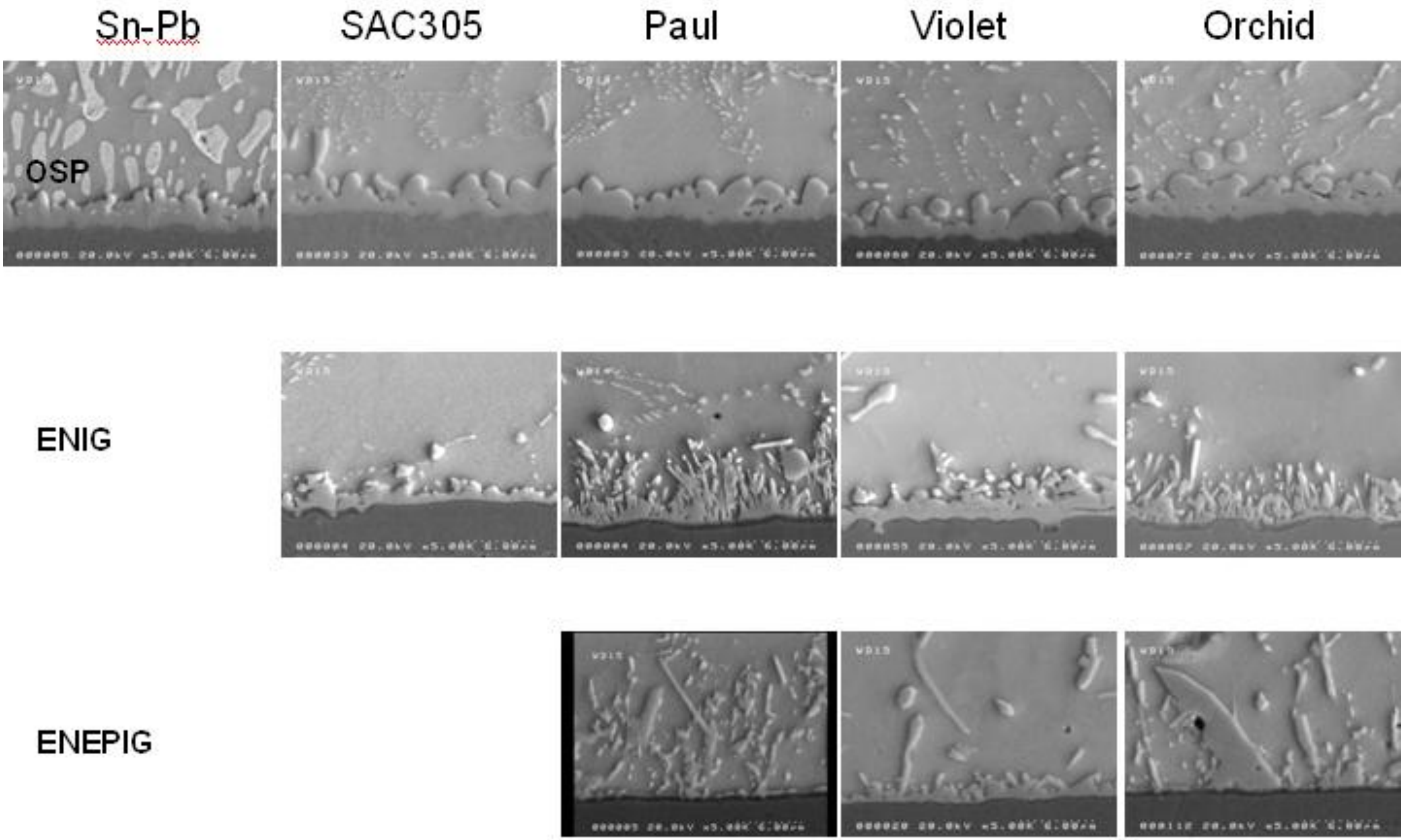

SEM, 5000x

QFP240: IMC Morphology

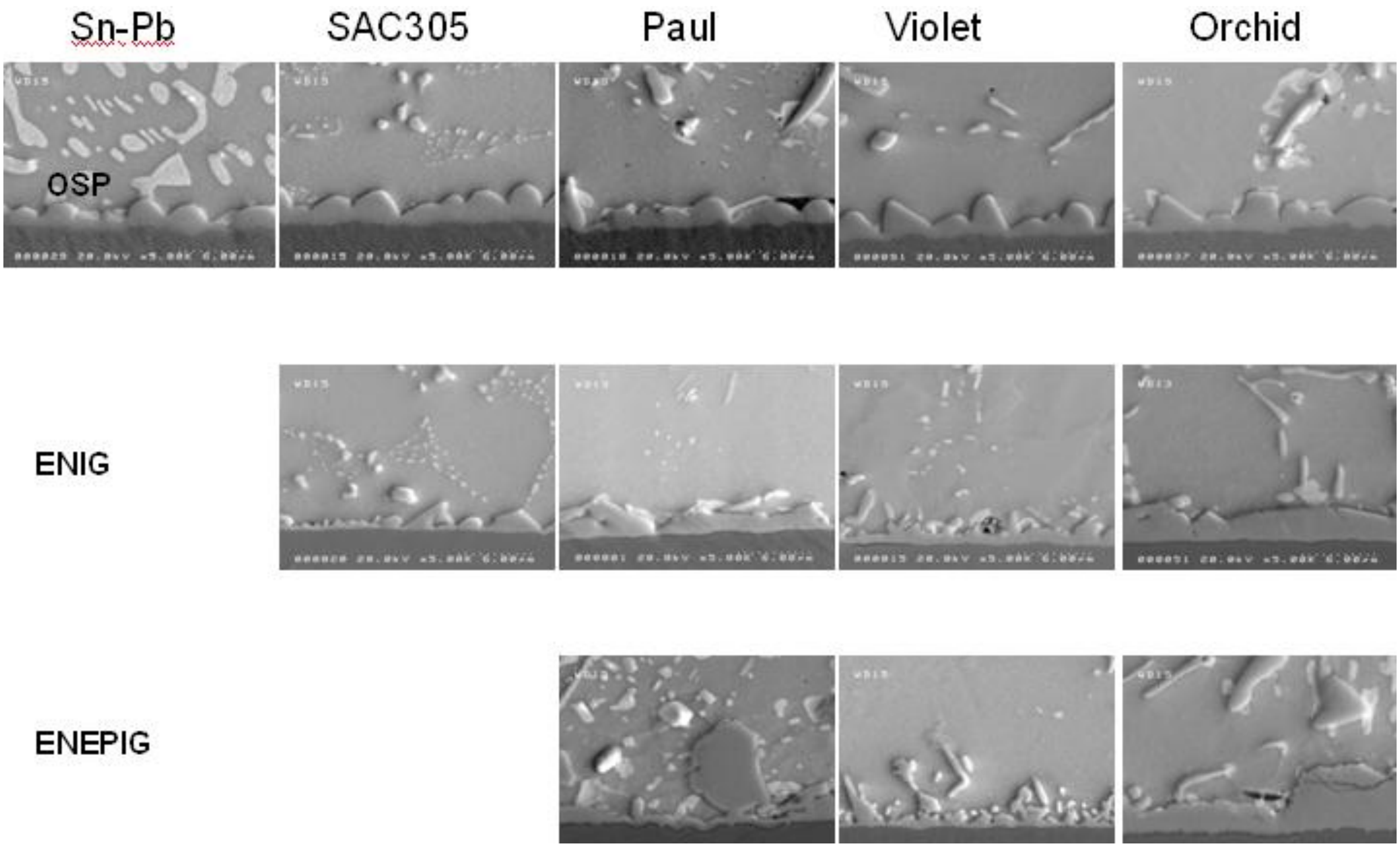

SEM, 5000x

Intermetallic Thickness and Morphology

- Solder joint properties depend on IMC thickness, type and morphology
- IMC thickness does not exceed 3.9µm
  - Exclude Paul and Orchid BGAs on ENEPIG –irregular and thick
- The morphology is deeply dependent on the IMC lattice and composition
  - Cu_6Sn_5 (η-phase) on OSP in SnPb and Pb-free solders
    - Nodule morphology
  - $Ni_{23}Cu_{33}Sn_{44}$ on ENIG and ENEPIG in SAC305 or Violet with Cu
    - Smooth cellular morphology
  - $(Ni,Cu)_3Sn_4$ on ENIG boards in Paul and Orchid alloys with no Cu
    - Sharp needle-like structure
  - $(Ni,Cu)_3Sn_4$ + Pd-based $MeSn_4$ on ENEPIG in Paul and Orchid alloys
    - Non-uniform, irregular shape and have needle–like morphology
- Only the Violet IMC layer has a regular proper shape on the ENEPIG finish

Intermetallic Thickness and Morphology

- Pd-based needles in QFP joints formed on ENEPIG
- A needle-like morphology causing stress concentration may reduce reliability

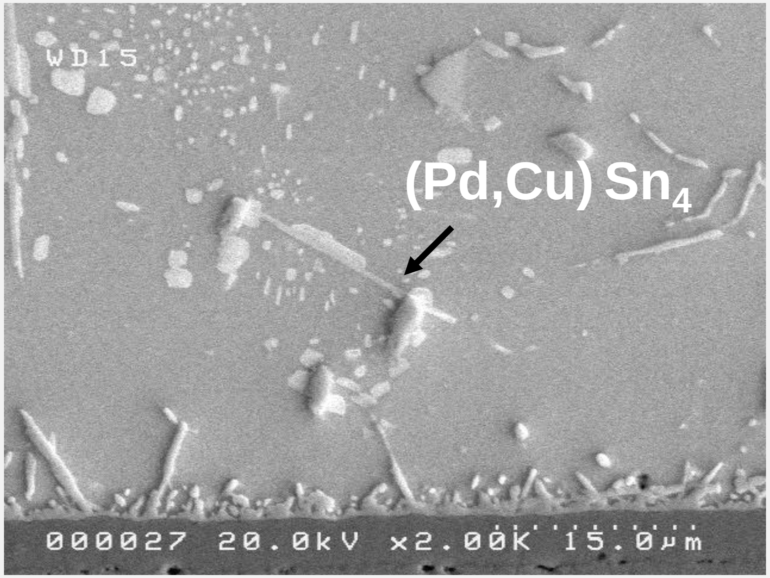

Element	Weight%	Atomic%
Cu K	1.1	2.0
Pd L	12.8	14.0
Sn L	86.1	84.0
Totals	100.0	

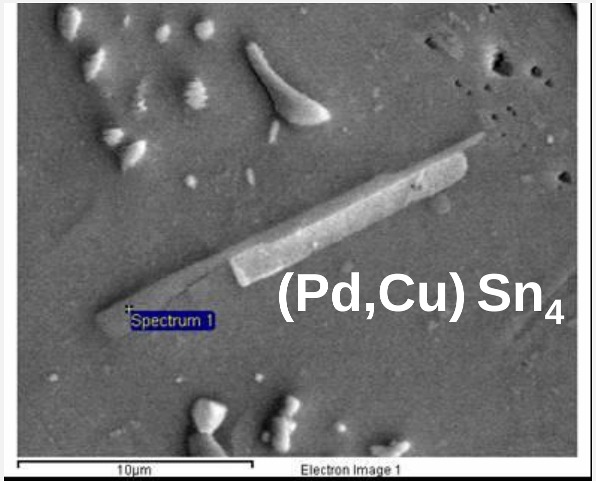

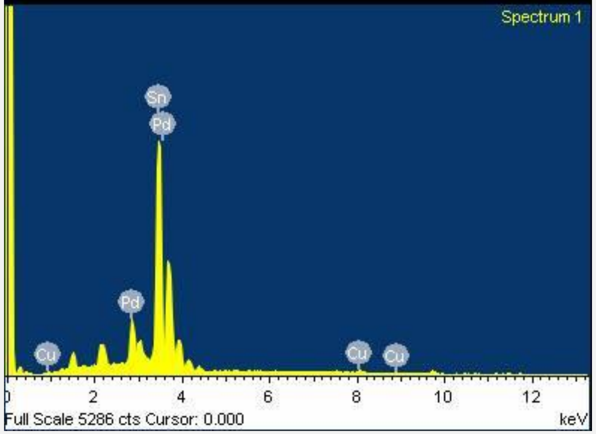

Test Strategy for Harsh Environment

- The solder interconnections are different under thermal cycling and mechanical shock loadings
- ATC target
  - -55°C to 125°C
  - 10°C/min ramp rate
  - 30 minute dwell at both extremes
  - 3000 cycles
- Vibration testing plan
  - 5G level and
  - 2G level
  - Resistance, strain and vibration recorded

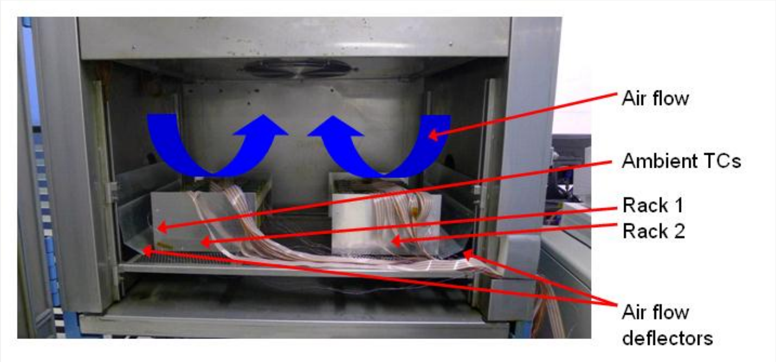

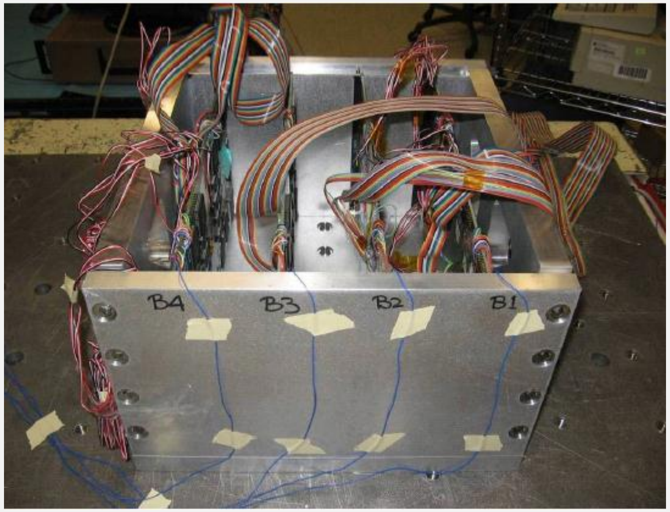

ATC Testing

- The actual profile
  - -58°C to 130°C
  - 38 minutes in a hot dwell
  - 39 minutes a cold dwell
  - 13 minute ramp
  - 103 minutes per cycle
  - 2001 cycles completed
- Analysis Tech STD-256 event detectors
- A failure recorded when the resistance increased to 300Ohms or more for at least 200ns
- Checked at room temperature to determine the location of failure

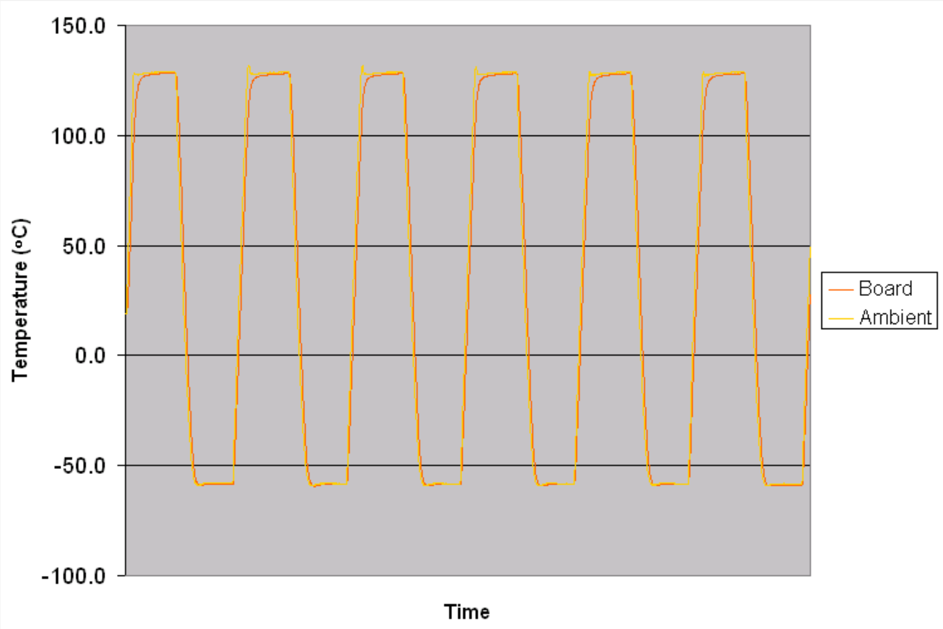

- 17 boards tested, 32 components monitored on each boards
- Selected failed components were cut from the board for detailed analysis
- The remaining components were returned to the chamber for further testing

ATC Results After 1548 cycles at -58° C to 130° C

Criterion:1000 cycles at -55° C to 125° C the Airspace qualification requirements

- 170° C Tg cells
  - No failures up to 1548 cycles, passed the requirements
  - All three Bi-containing alloys, SAC305 and SnPb assembled on
  - OSP, ENIG and ENEPIG
- 150° C Tg cells
  - Some failures on OSP finished boards
  - SAC305 assemblies failed before the 1000 cycle criterion
  - SnPb and Paul alloys passed 1000 cycles at -55° C to 125° C criterion
  - Violet and Orchid did not fail
  - No failures on ENIG and ENEPIG boards
- The failures are caused by via failures
- Early failure of vias in SAC305 are attributed to the higher process temperatures

ATC Results After 1548 cycles at -58° C to 130° C

Component type	Cycles to failure, -55° C to 125° C	Solder paste	Board finish	Tg
SSOP48	853	SAC305	OSP	150
SSOP48	1072	Paul	OSP	150
SSOP48	1255	Paul	OSP	150
SSOP48	1290	Paul	OSP	150
SSOP48	1256	SnPb	OSP	150
SSOP48	1287	SnPb	OSP	150
QFP240	485	SAC305	OSP	150
QFP240	1062	Paul	OSP	150
QFP240	1275	Paul	OSP	150
QFP240	1287	Paul	OSP	150
PLCC84	1005	Paul	OSP	150
PLCC84	1464	Paul	OSP	150
PLCC84	1504	Paul	OSP	150
352BGA	504	SAC305	OSP	150
352BGA	598	SAC305	OSP	150
352BGA	1043	Paul	OSP	150
352BGA	1067	Paul	OSP	150
352BGA	1341	SnPb	OSP	150

Confirmed via failures

Failure Analysis After ATC

- Failure analysis on all 18 failures
- Failed components cut off the boards
  - failure electrically determined
- Cross-sections through
  - solder joint and
  - related via

- No failure in solder joints
  - SSOP48, QFP240, and PLCC84 – not even micro cracks
  - BGA352 – tiny micro cracks

- Circular cracks in via
  - Responsible for open circuits in OSP cells
  - Arrested in the ENIG and ENEPIG cells by the Ni barrier layer

- ATC is in progress and more work will be done to understand the difference between the alloys

Failure Analysis

BGA352

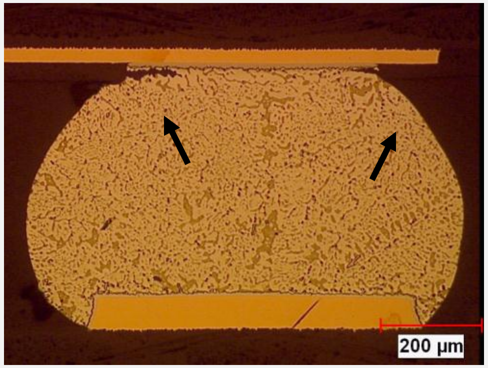

SnPb, 1257 cycles

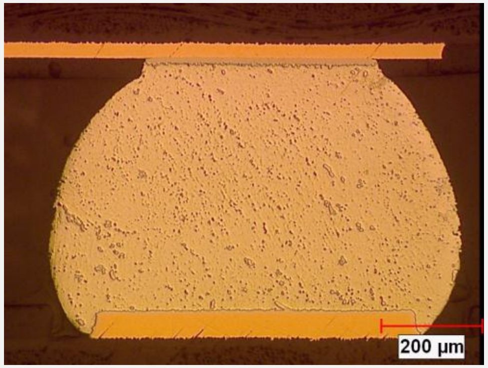

Paul, 1067 cycles

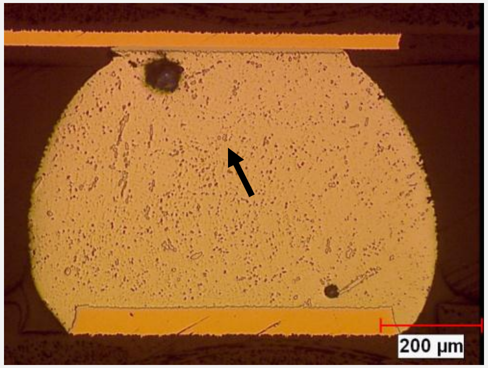

Paul, 1043 cycles

SSOP48

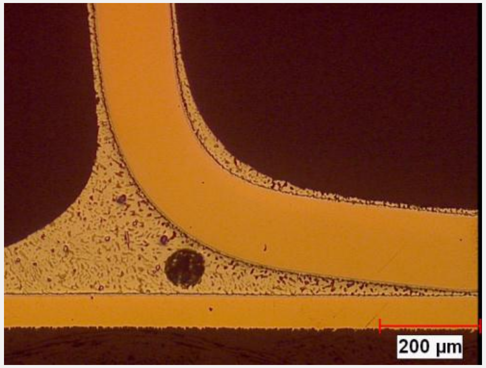

SnPb, 1257 cycles

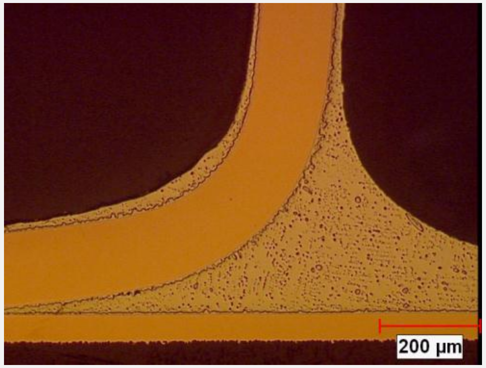

Paul, 1255 cycles

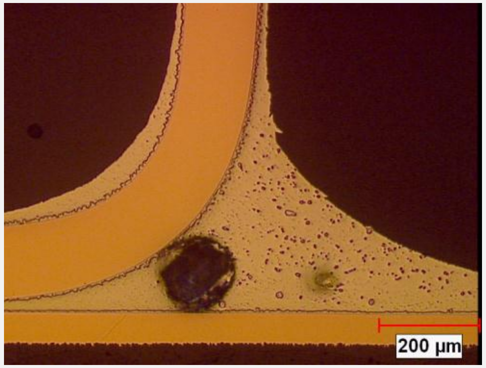

SAC305, 850 cycles

Failure Analysis

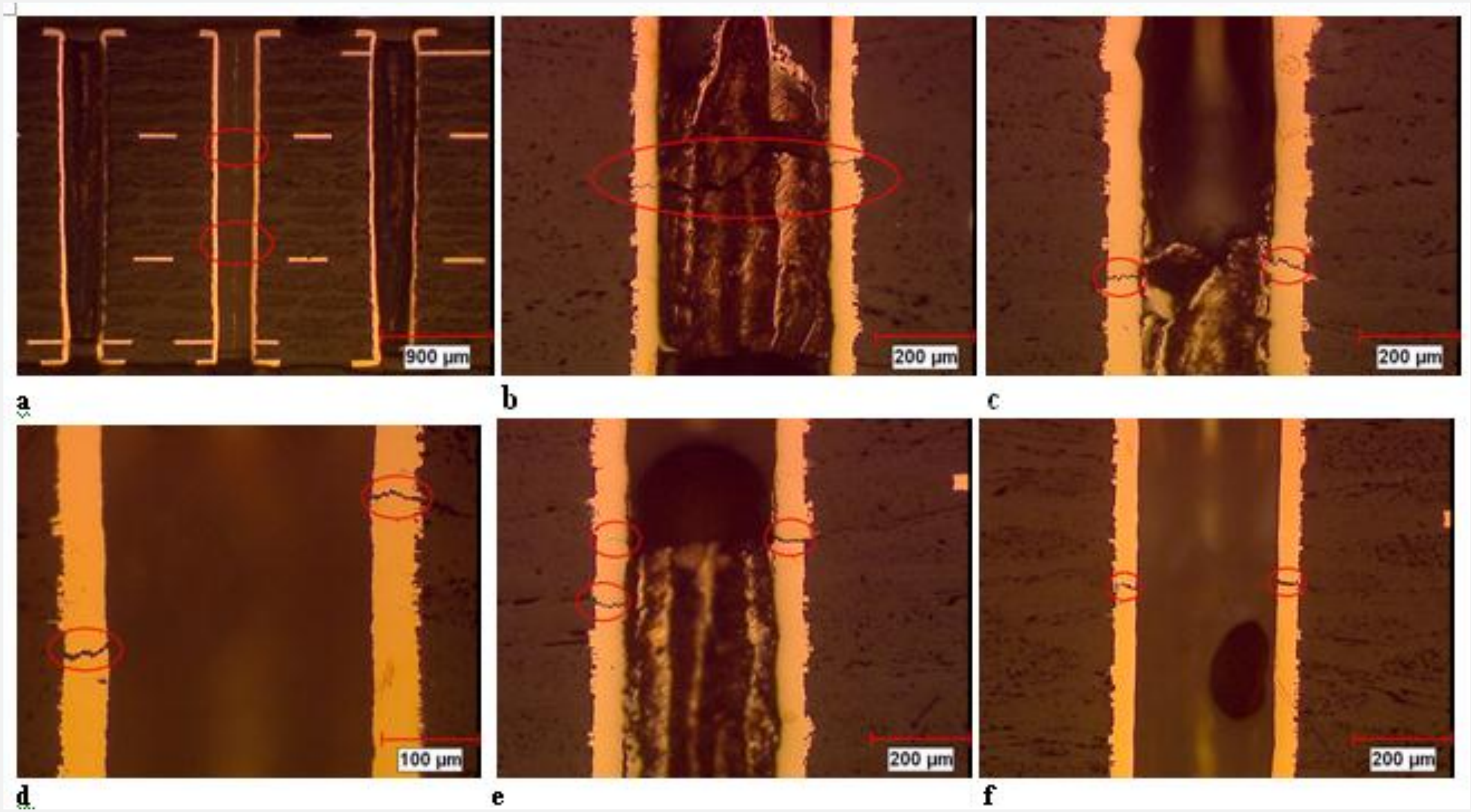

Summary and Conclusions

Screening experiments on the manufacturability and reliability of the lower melting Pb-free alloys that may satisfy the Aerospace requirements are in progress.

The following results and conclusions may be made at this time.

- Three Bi-containing alloys: Sn3.4Ag4.8Bi (Paul) and two reduced Ag content variations, with and without Cu, Sn2.25Ag0.5Cu6Bi (Violet) and Sn2Ag 7Bi (Orchid), were selected.
- Honeywell test vehicles were assembled using these alloys with the process temperature about 10° C below SAC305.
- Two board materials with high Tg and normal Tg were used. The boards were finished with OSP, ENIG, and ENEPIG.
- No problems related to the manufacturability were detected. Experimental alloys had better wetting and less voiding than SAC305. The joints had a proper shape comparable to both SnPb and SAC305.

Summary and Conclusions: Microstructural Analysis

- All three Bi-containing alloys formed excellent joints on OSP finish. The interfacial intermetallic layer is comparable to SnPb in thickness and shape and thinner than in SAC305
- Sn3.4Ag4.8Bi (Paul) and Sn2Ag 7Bi (Orchid) are not fully compatible with ENIG and ENEPIG, forming irregular and/or thicker interfacial intermetallic than SAC305. This is attributed to the lack of Cu in these alloy compositions.
- The alloy with Cu, Sn2.25Ag0.5Cu6Bi (Violet), is compatible not only with OSP, but also with ENIG and ENEPIG, and forms excellent solder joints with uniform intermetallic layers on both ball grid array and leaded components
- On the ENEPIG finish, Pd-containing needle-shaped intermetallic particles are present in solder joints. These particles may cause solder joint embrittlement. The ENEPIG finish must be fully qualified for Aerospace industry acceptance.

Summary and Conclusions

- There was no solder joint failure on both high and normal Tg boards after 1548 cycles at -55° C to 125° C completion.
- However, there were via failures in normal Tg boards with OSP finish, assembled using SAC305, Sn3.4Ag4.8Bi (Paul), and SnPb solders. Of these via failures on normal Tg OSP finished boards only the SAC305 cell did not meet the Aerospace qualification requirement of 1000cycles.
- Therefore, all three experimental alloys Paul, Violet, and Orchid showed excellent performance in harsh environment thermal cycling.
- Further ATC and vibration testing are in progress. More results will be reported upon the program completion.

Future Work

- -58° C to 130° C cycling and vibration are in progress
  - Results and analysis of ATC 3000 cycles
  - Vibration testing results and analysis

- These screening test results will be shared to help launch a new NASA consortium phase 3 project focused on the requirements of the Aerospace industry.

Acknowledgements

The authors would like to thank the following individuals from Celestica: Russell Brush, Alon Walk, Kangwon Lee, Veseyathaas Thambipillai for ATC testing and data analysis; Jie Qian for sample preparation; Jose Traya and Michael Emery for test vehicle assembly; Suthakaran Subramaniam and Michelle Le for vibration testing; and Dr. John Vic Grice, Honeywell Corporate consulting statistician, who helped design the experimental matrix.